



HAL
open science

The influence of plant root systems on soil erodibility and infiltration processes in mountain ecosystems

Manon Bounous

► **To cite this version:**

Manon Bounous. The influence of plant root systems on soil erodibility and infiltration processes in mountain ecosystems. Systematics, Phylogenetics and taxonomy. 2019. hal-02794387

HAL Id: hal-02794387

<https://hal.inrae.fr/hal-02794387>

Submitted on 5 Jun 2020

HAL is a multi-disciplinary open access archive for the deposit and dissemination of scientific research documents, whether they are published or not. The documents may come from teaching and research institutions in France or abroad, or from public or private research centers.

L'archive ouverte pluridisciplinaire **HAL**, est destinée au dépôt et à la diffusion de documents scientifiques de niveau recherche, publiés ou non, émanant des établissements d'enseignement et de recherche français ou étrangers, des laboratoires publics ou privés.



Université de Montpellier & Montpellier SupAgro

Master Mention " Biodiversité, Ecologie, Evolution, B2E "

Parcours « EcoSystèmeS »

Research Project:
The influence of plant root systems on soil erodibility and infiltration processes in mountain ecosystems

By
Manon BOUNOUS
Stage de M2
Defense the 12/06/2019

Under the supervision of

Catherine ROUMET, Chargée de recherche - CNRS
UMR Centre d'Ecologie Fonctionnelle et Evolutive (CEFE)

And

Alexia STOKES, Directrice de recherche - INRA
UMR botAnique Modélisation de l'Architecture des Plantes (AMAP)



Résumé

1. *Contexte* Les écosystèmes de montagne prodiguent d'importants services écosystémiques de régulation et d'atténuation de l'érosion. Ces processus sont largement déterminés par le type de communauté végétale, qui évolue avec l'altitude. L'impact des changements de communautés végétales sur les processus avec l'altitude reste peu connu.

2. *Méthodes* En juin 2018, une étude a été réalisée le long d'un gradient d'altitude de 1000 m (1400 – 2400m) dans le Massif de Belledonne (Alpes françaises). A six altitudes et sous trois espèces ligneuses (*Picea abies*, *Juniperus communis* et *Vaccinium myrtillus*), ont été mesurés la biomasse de racine et les traits racinaires à l'échelle de la communauté et deux processus du sol liés à l'atténuation de l'érosion : l'érodibilité et l'infiltration de l'eau. Cette étude vise à tester les relations environnement – trait – processus en considérant la végétation, le climat et le sol.

3. *Résultats* En altitude, où la température et la fertilité sont moindres, les communautés produisent plus de racines fines ayant une longueur spécifique élevée ; une stratégie permettant d'acquérir plus de ressources pendant la courte saison de croissance. Les racines ont également des tissus plus denses afin d'assurer la survie pendant la période défavorable. L'érodibilité et l'infiltration diminuent avec l'altitude, et sont expliquées par les caractéristiques du sol et dans une moindre mesure par les racines.

4. *Perspectives* L'étude de ces processus pourrait être améliorée par la prise en compte de la diversité et de l'activité des animaux et micro-organismes du sol.

Mots clés Alpin - Changement climatique – Gradient altitudinal - Infiltration de l'eau – Stabilité des agrégats - Traits racinaires

Abstract

1. *Context* Mountain ecosystems provide important regulation ecosystem services such as erosion mitigation. These processes are largely determined by the type of plant community, that is modified with elevation. The influence of plant community changes on soil processes with elevation is still poorly known.

2. *Methods* In June 2018, a study was carried out along an elevational gradient (1400 – 2400m) in the Massif de Belledonne (French Alps). At six altitudinal levels and under three keystone species (*Picea abies*, *Juniperus communis* and *Vaccinium myrtillus*), we measured root biomass and fine-root traits at the community level and two soil processes linked to erosion mitigation: erodibility and infiltration. We aimed to test environment-trait and trait-processes relationships considering vegetation, climate and soil.

3. *Results* At high elevation, where temperature and fertility are lower, we observed an increased production of roots with high absorptive capacity (small diameters and high specific root length), a strategy favouring belowground resource acquisition in the short growing season. Roots also demonstrated increasing persistence through the production of greater tissue density. Erosion mitigation decreased along elevation, and were explained by both soil properties and – to a lesser extent – root characteristics.

4. *Perspectives* The understanding of these processes would be improved by the study of soil animal and micro-organisms diversity and activity.

Key words Aggregate stability - Alpine – Climate change – Elevational gradient - Root traits – Water infiltration

Acknowledgments

Firstly and foremost, I would like to thank Catherine Roumet and Alexia Stokes for their astounding help and for their extraordinary support in this thesis process. I would like to thank them for their inestimable advices and time, and for the independence and confidence given to me. Thanks to have accepted to help me in this incredible experience.

Thanks to Zhun Mao and Luis Merino-Martin for fruitful discussions about statistics and great feedbacks. Thanks to Monique Weemstra for her great encouragements, support and friendship. Thanks to Beatriz Marín-Castro for her valuable help in performing infiltration calculations.

A special thanks to the AMAP and CEFE teams for welcoming me in their labs. This project would have been impossible without the ECOPICS team and the memorable field campaign we experienced together in Chamrousse. Project funding was provided by the French Government ANR project ECOPICS: Belowground ecosystem services in plant communities along elevational and landuse gradients in France and Mexico (ANR-16-CE03-0009-01).

1. Introduction

Mountain ecosystems possess a high diversity of habitats and species endemism (Körner, 2007), as well as contributing to ecosystem services such as water and air quality and soil protection (Stokes *et al.*, 2014). These ecosystems are characterized by high elevation and steep slopes, making them susceptible to soil erosion and shallow landslides, especially during snowmelt and heavy rainstorms. Therefore, managing soil conservation in mountainous regions is a priority for stakeholders aiming to improve the provision of ecosystem services. Soil erosion and resistance to landslides are influenced significantly by the structural stability of soil (erodibility, or aggregate stability, Le Bissonnais, 1996 ; Barthès & Roose, 2002) and the capacity of rainfall to infiltrate soils (Lado *et al.*, 2004). Water infiltration occurs through the pore network and is determined largely by the quantity, intensity and speed of precipitation (Marín-Castro *et al.*, 2017 ; Nespoulous *et al.*, 2019). On vegetated slopes, plant communities can influence significantly soil structure. However, our understanding of the relative contribution of vegetation, roots, litter and soil characteristics on structural stability and infiltration is not yet fully understood, where dominant and keystone plant species can have a major effect on above- and belowground ecosystems processes.

The influence of vegetation on soil erodibility can be major (Walsh & Voigt, 1977 ; Ghestem *et al.*, 2011 ; Le Bissonnais *et al.*, 2018). First, the plant canopy intercepts raindrops and regulates the intensity and speed of water runoff (Dunne *et al.*, 1991). Vegetation also provides organic matter to the soil; a thick litter layer and high root density improve soil structural stability and reduce surface runoff (Bast *et al.*, 2014 ; Marín-Castro *et al.*, 2017). Plant root systems create an interconnected macropore network whereby coarse roots (>2 mm in diameter) act as preferential channels for water infiltration (Gerke & Kuchenbuch, 2007 ; Nespoulous *et al.*, 2019). Roots also contribute to the formation and stabilisation of soil aggregates and a matrix of pore space (Six *et al.*, 2002 ; Rillig *et al.*, 2015). Fine roots (<2 mm) characteristics favour soil aggregate stability as they enmesh fine particles into stable aggregates and produce carbon-rich exudates acting as binding agents (Tisdall & Oades, 1982 ; Erktan *et al.*, 2016 ; Le Bissonnais *et al.*, 2018 ; Poirier *et al.*, 2018). Fine roots comprise (i) ephemeral absorptive roots that are nitrogen (N) rich, favouring mycorrhizal colonization and performing nutrient and water uptake, and (ii) transport roots that are thicker, more lignified and longer lived performing transport and storage functions (McCormack *et al.*, 2015; Freschet & Roumet, 2017). Positive relationships have been observed between the quantity of thin roots with higher specific root length and tissue density and lower N content, and aggregate stability as they promote exudation and mucilage production acting as binding agents (Erktan *et al.*, 2016; Le Bissonnais *et al.* 2018) and water infiltration (Nespoulous *et al.*, 2019). Therefore, plant communities should influence strongly soil loss and conservation on mountain slopes, and as communities shift along an elevational gradient, so should these changes be reflected belowground.

Environmental gradients can be used as a space-for-time substitution to infer species' effects on ecological systems (Fukami & Wardle, 2005). In particular, after latitude, elevational gradients are the most structuring factor of living communities (Körner, 2007), and through climatic, edaphic and biotic effects, determine plant community composition and potential ecosystem trajectories. As species are present in different abundances along an elevational gradient, it is possible to infer their biophysical effects on a plant community, both above- and belowground. Plant species traits differ along elevational gradients, to better survive long, cold winters and extreme variations in temperature. Species from alpine climates have specific adaptations to cope with low soil fertility and cold temperatures. They usually exhibit thinner

roots and have a higher specific root length (SRL) compared with low-altitude plants (Körner & Renhardt, 1987 ; Pohl *et al.*, 2011 ; Freschet *et al.*, 2017). Higher SRL and, thus, more efficient investment of carbon for spatial soil exploration, is considered to compensate for the lower availability of nutrients at high elevation or as a compensation for poorer mycorrhization (Körner, 1998). Roots of alpine species also have higher tissue density (RTD) and tensile strength (Pohl *et al.*, 2011). These two traits are associated with the conservation of resources in long lived tissues; they enable the plant to withstand uprooting and to remain anchored in the soil, e.g. during grazing, intense rainfall (Ennos & Pellerin, 2000) or at times of soil movement (Jonasson & Callaghan, 1992); they also contribute to hold aggregates together physically. Whether variation of root traits along elevational gradients is similar at the species and at the community level remains unclear. Changes in the community root traits indeed result from the replacement of species with different trait values (interspecific variation), from within-species changes in trait values (intraspecific variation) or to a combination of these two sources of variability (Garnier *et al.* 2004). Along altitudinal gradients root traits measured at the community level are thus expected to be influenced by the dominance of tree species with coarse roots at low elevation and by the dominance of herbaceous species with thinner roots at high elevation. Therefore, these differences in traits at the community level should also affect soil processes, with subsequent effects on soil loss and conservation.

Here, we used an elevational gradient in the French Alps to better understand how changes in plant community composition affect soil structural stability and rainfall infiltration. Increasing elevation along this gradient was associated with a decline in air temperature and soil fertility and an increase in precipitation. Vegetation shifted from mixed forest to prairies with increasing altitude. We chose to focus on plant communities associated with keystone species. Keystone species have a disproportionately large effect on the community relative to their abundance (e.g., *Picea abies*, Bjune *et al.*, (2009), *Vaccinium myrtillus*, Nybakken *et al.*, (2013) and certain *Juniperus* species Garcia *et al.*, (2014)). Keystone species are especially important when managing a site with regard to erosion or shallow landslides, because of their importance in the ecological trajectory of an ecosystem (Stokes *et al.*, 2014). Specifically, we tested the following hypotheses: (1) the evergreen conifers, *P. abies* and *J. communis* favour water infiltration because they protect the soil surface from rain drop impacts and splash erosion and induce the formation of a deep litter layer and have higher proportion of coarse roots, whereas the deciduous dwarf shrub *V. myrtillus* reduces rainfall infiltration and aggregate stability because they produce a shallow litter layer and thinner roots; (2) at high elevation, where plant growth is limited by temperature and low soil fertility, plants allocate more biomass to fine roots in order to favour resource acquisition; fine roots are also expected to have a higher tissue density and lignin concentration to better resist the biophysical environment that is subjected to extreme variations in climate and substrate disturbance e.g. snowmelt and storms; (3) at higher elevations, soil erodibility and water infiltration should decrease because the litter layer is thinner and plant root density is decreased. By addressing these hypotheses in combination, we aimed to advance our understanding of how soil erodibility and infiltration under different types of plant communities could be explained by plant root traits or by other environmental variables.

Table 1: Physical and climate characteristics of elevational levels (means \pm confidence interval). Soil depth was measured once in a pedological pit per altitudinal level. Climate data are from AURELHY model. For abbreviations refer to Table S5.

Elevation level	Measured altitude (m a.s.l.)	Coordinates (hddd°mm.mmm')	MAT (°C)	GSL (month)	MAP (mm)	ETP (mm)	AI	Soil Depth (cm)	Vegetation stage
1400	1366 \pm 13	45,0815499 5,85799998	8.46 \pm 0.17	7,5 \pm 0,1	1024 \pm 41	663 \pm 9	1,6 \pm 0,1	92	Mountain
1600	1601 \pm 11	45,0925691 5,86910275	7.27 \pm 0.72	6,7 \pm 0,1	1066 \pm 20	612 \pm 9	1,8 \pm 0,1	97	Subalpine
1800	1799 \pm 17	45,1083147 5,89275234	8.08 \pm 0.50	7,3 \pm 0,1	1110 \pm 7	593 \pm 11	1,9 \pm 0,1	85	Subalpine
2000	1971 \pm 9	45,1173978 5,90282301	5.74 \pm 0.66	6,2 \pm 0,1	1155 \pm 12	535 \pm 9	2,2 \pm 0,1	95	Subalpine
2200	2208 \pm 17	45,1273033 5,92293165	3.79 \pm 0.10	5,0 \pm 0,1	1205 \pm 20	485 \pm 9	2,5 \pm 0,1	49	Alpine
2400	2405 \pm 15	45,1295105 5,9303625	5.72 \pm 0.20	6,1 \pm 0,3	1187 \pm 40	485 \pm 11	2,5 \pm 0,1	80	Alpine

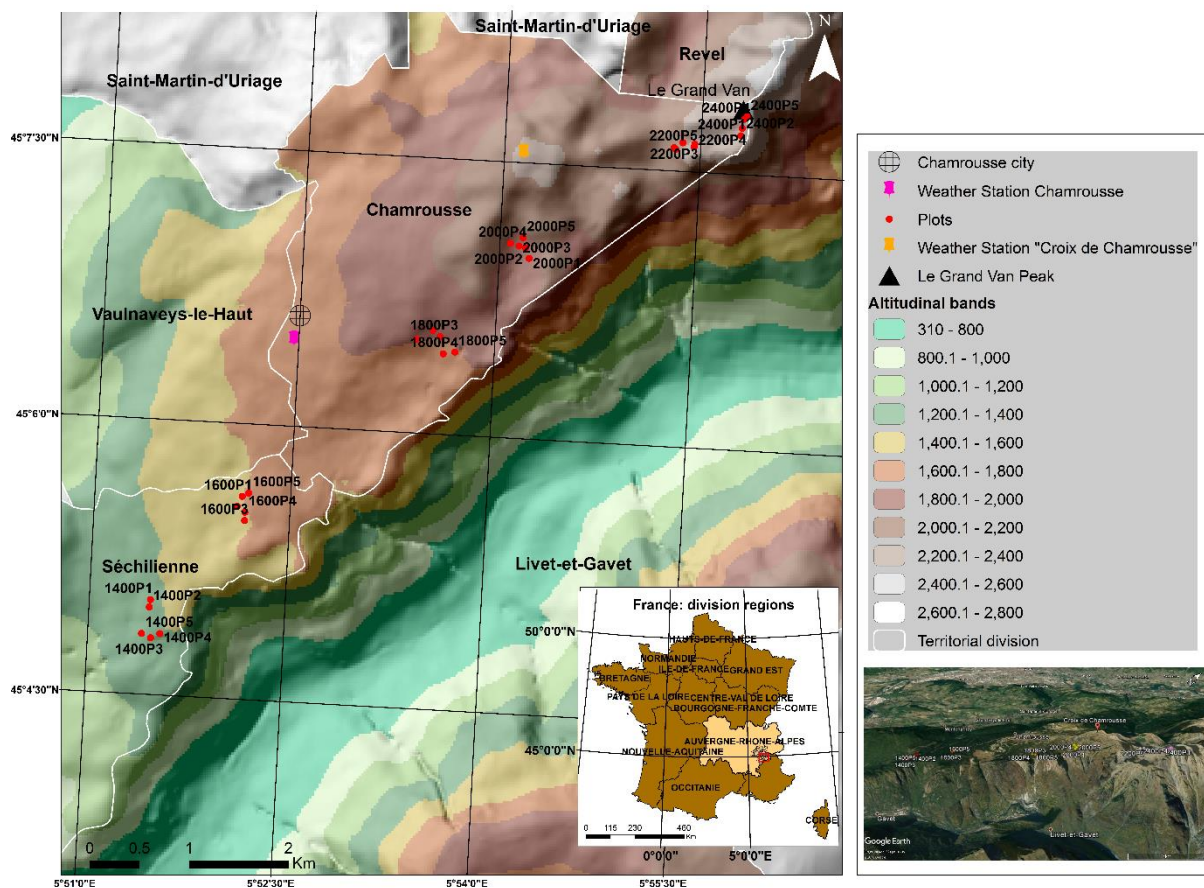


Figure 1: Plot locations (red dots) along the elevational gradient ranging from 1400 – 2400m in the Massif de Belledonne, France. Colours reflect 200m wide altitudinal bands, ranging from green (lowest altitudes) to brown-grey (highest altitudes). Two weather stations (pink and orange dots) were located nearby.

2. Material and Methods

2.1. Study site

This study was conducted along an 8 km elevational gradient located in Massif de Belledonne within the Chamrousse municipality (Isère, France, N 45° 7' 1" E 5° 53' 35") close to Grenoble (Figure 1). The gradient ranged from 1400 to 2400 m above sea level (a.s.l.), on a South-East facing slope. Along the elevational gradient, we chose experimental plots at six altitudinal levels situated at a distance of 200 altitude m from each other (Figure 1). The treeline was situated between 2000 and 2100 m a.s.l. and was defined by the replacement of acidophilous *Picea abies* forests of the montane levels (Vaccinio myrtilli-Piceetea abietis) by arctico-alpine heath (Loiseleurio procumbentis-Vaccinieta microphylli, Figure 1, Table 1, Bardat *et al.*, 2004). Bedrock along the gradient was composed of variscan metamorphic rocks and ophiolitic complexes and the soil was on average 83 cm deep (Table 1).

2.2. Climatic data

Climatic data were calculated at each elevation using the meteorological Aurelhy model at a resolution of 1 km (Bénichou & Lebreton, 1987 ; Piedallu *et al.*, 2013 ; Piedallu *et al.*, 2016). Over the 2004-2014 period, mean annual temperature (MAT) was 8.46 ± 0.17 °C at 1400 m and 5.72 ± 0.20 °C at 2400 m, i.e. a decrease of 0.28 °C for every 100 m of altitude occurred (Table 1). The length of the growing season in 2018 decreased from 7.5 ± 0.1 at 1400 m to 6.1 ± 0.2 months at 2400 m (Table 1). Mean annual precipitation (including snow, MAP) was greater at high altitudes (increasing from 1024 ± 41 to 1187 ± 40 mm), and mean annual evapotranspiration decreased from 663 ± 9 to 485 ± 11 mm (Table 1). The aridity index, calculated as following: $AI = \frac{MAP}{ETP}$ where ETP is the mean annual evapotranspiration increased thus from 1.6 ± 0.1 at 1400 m to 2.5 ± 0.1 at 2400 m, corresponding to a decrease in aridity at high elevation.

2.3. Sampling design

In June 2018, after snow melt, five plots (20 x 20 m) were selected within each elevational level at an average distance of 100 m from each other for plots below the treeline and 50 m for plots above the treeline, so avoiding issues with pseudo-replication (Figure 1). The plots had a South-West orientation (azimuth of $220 \pm 26^\circ$) and a mean angle of $17.5 \pm 2.3^\circ$ from the vertical. Areas with visible bedrock or signs of waterlogging were avoided. The plots were chosen so that two or three of keystone species were present: *Picea abies* (Pinaceae, L. H., Karst, 1881), *Vaccinium myrtillus* (Ericaceae, L., 1753) and the only *Juniperus* species present: *Juniperus communis* (Cupressaceae, L., 1753, Figure 2). We assumed that when the species was abundant within a plot, it had a strong long- term influence on both biotic and abiotic properties. The three species differed in their growth form and elevational distribution along the gradient. *P. abies*, a tall evergreen conifer, was the most dominant tree species below the treeline and its percentage cover decreased regularly from 31 ± 4 % at 1400 m to 3 ± 2 % at 2000 m (Figure S10). *J. communis*, a prostrate evergreen shrub, was present from 1800 m to 2400 m, and was the most abundant shrub above the treeline with a mean percentage cover of 9 ± 4 % (Figure S10). *V. myrtillus*, a deciduous dwarf shrub was present at all elevations and was more abundant below (17 ± 5 %) than above (6 ± 3 %) the treeline (Figure S10). Therefore, only *V. myrtillus* and *P. abies* were present at 1400 and 1600 m, and only *J. communis* and *V. myrtillus* were present at 2200 and 2400 m (Figure 2). A botanical survey of both near-ground and tree strata was performed on each 20 x 20 m plot. Vascular plants were identified using

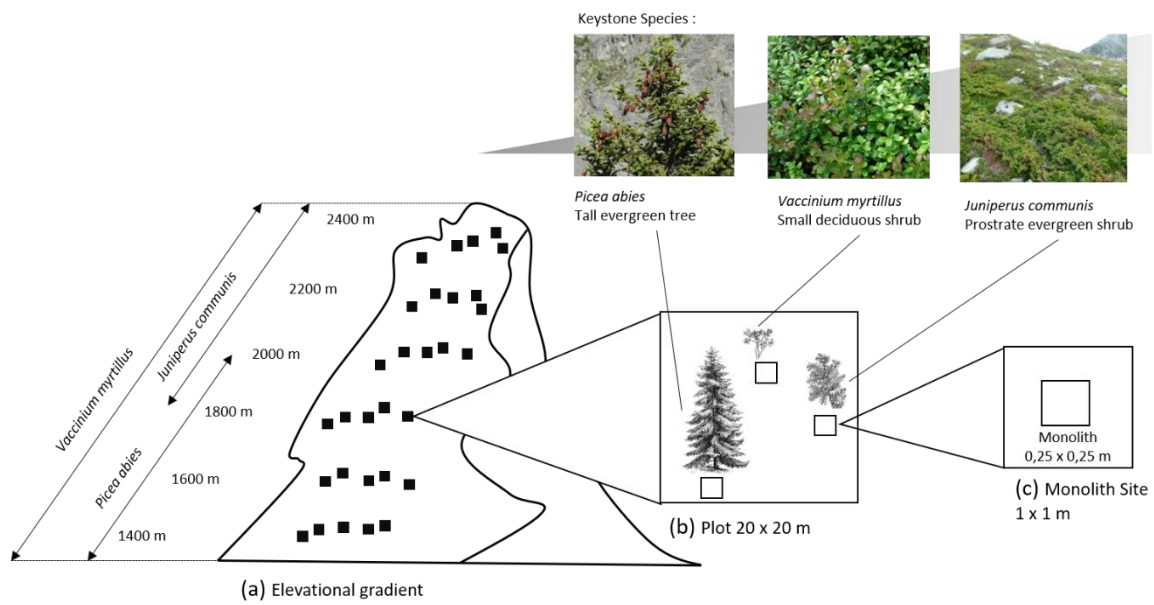


Figure 2: Sampling design along the elevational gradient. (a) Six elevational levels, each situated at 200m from each other, were located along the gradient, ranging from 1400m to 2400m. Five plots (20m x 20m) containing two or three keystone species were located at each altitude. (b) Under the canopy limit of the keystone species, a 1mx1m botanical survey was performed. (c) In the centre of this quadrat, a soil monolith (0.25m x 0.25m x 0.15m) was extracted.

two floras (Flore Forestière Française, Montagnes, Rameau *et al.*, 1999 and Flora Helvetica, Laufen *et al.*, 2001, Figure S10). Within each plot, one adult and well-developed individual of each species was selected. At the limit of the plant's canopy on the downslope side, an area (0.25 m width x 0.25 m length, hereafter termed 'monolith site') was chosen for a detailed study of plant and soil characteristics (Figure 2). First, a botanical survey was performed on a 1.0 x 1.0 m quadrat centred on the 0.25 x 0.25 m monolith site, using the same method utilised previously at the 20 x 20 m plots. Simpson diversity index (S) was calculated as following: $S = \frac{1}{\sum_{i=1}^n p_i^2}$, where p_i is the proportion of individuals of one particular species and n the number of species.

2.4. Water infiltration through soil

Infiltration tests were carried out on a flat patch of soil within a distance of 1.0 m to each monolith site. We used a constant head single ring infiltrometer (Marin-Castro *et al.*, 2016). Before each test, the litter layer was removed and a metal ring (0.15 m diameter and 0.05 m deep) was inserted directly into the topsoil. This large ring increased the sampling area and allowed the capture of microheterogeneity in soil infiltration (Wu *et al.*, 2017). Water was poured into the 1.40 dm³ column. We measured the speed at which 0.08 dm³ of water entered the soil. We repeated the test 5-7 times, until a quasi-steady infiltration rate had been achieved. To improve robustness in the data set, we calculated mean values using data from the final two to three infiltration tests performed. Hydraulic conductivity (Kfs) of the quasi-steady phase was estimated from the slope of the upper linear part of the mean cumulative infiltration calculated using equation 1 (Wu & Pan, 1997 ; Wu *et al.*, 1999):

$$Kfs = \frac{A}{af} \quad \text{Eq. (1)}$$

Where Kfs (cm.h⁻¹) is the field saturated hydraulic conductivity, A the slope of the mean square regression of cumulative infiltration (cm.h⁻¹), a is a dimensionless constant (0.9084) and f a dimensionless correction factor depending on soil properties and ring geometry calculated as: $f = \frac{H+1/\alpha}{G^*}$ where H is the ponded depth in the ring, or constant pressure head, recorded in the field before each infiltration test (cm), α is a parameter depending on the soil texture, here for structured soil with clay and silt content the value of 0.12 cm⁻¹ as proposed by (Elrick & Reynolds, 1992) was used, and G^* is a shape factor defined as $G^* = d + \frac{r}{2}$ where d is the inserted depth of the ring (50 mm) and r the ring radius (150 mm).

2.5. Excavation and dissection of monoliths

At the monolith site, a 0.25 x 0.25 m square of soil was cut to a depth of 0.15 m using a knife. If stones impeded the cutting, a new square of soil was cut several centimetres away. A soil monolith (0.25 x 0.25 x 0.15 m) was then excavated using a metal frame driven by a heavy hammer. Any large roots were cut with a saw if necessary. A shovel was placed underneath the monolith to lift it out, it was then placed in a plastic tray and divided longitudinally. A total number of 70 monoliths were selected (six elevations x five plots x two to three keystone species per elevation). After the extraction of the monolith, the thickness of the litter layer was recorded on the three uppermost sides of the resulting pit in the ground. A cylinder of soil (115.89 cm³) was extracted next to each monolith site to a depth of 0.07 m, dried at 105°C and weighted to determine the bulk density (g.cm⁻³). Two additional soil samples (approximately 300 g in weight) were collected for soil aggregate stability measurements at two depths (topsoil: 0-0.25 m and subsoil: 0.25-0.50 m), with a small shovel to preserve the soil structure.

Samples were stored in rigid boxes, and air-dried in a well-ventilated atmosphere for four weeks prior to performing the stability tests (see section 2.8.).

Each monolith was immediately dissected in the field. Stone volume was determined on the whole monolith, and roots were collected from on one half of the monolith. At 2200 and 2400 m, when shallow bedrock or superficial stones impeded the use of the frame, a shovel was used to excavate the monoliths whose length, width and depth (cm) were recorded to calculate its volume. When the shape of the monolith was not cubic, its volume was determined by water displacement. The volume of stones and/or very coarse roots (> 5 mm in diameter) in these monoliths was measured to calculate the volume of soil available for root growth (dm^3) by water displacement using a graduated cylinder filled with water.

After monolith dissection had terminated, the roots were placed in moisten plastic bags and stored in an icebox before being washed at the lab the following day. A sample of soil (approximately 500 g), was pooled from several smaller samples randomly taken from each monolith. Pooled samples ($n = 70$) were air dried and sieved to 2 mm for further physical and chemical analyses (see section 2.7.).

2.6. Root trait measurements

Roots from each monolith were carefully washed in the lab and were spread in a tray filled with water to remove the remaining soil with tweezers. These roots represent a mixture of roots of the different species present in the plant community at the monolith site. They were sorted into four categories according to their diameter and functionality: rhizomes, very coarse roots with a diameter > 5 mm, coarse roots with a diameter between 2 - 5 mm and fine-roots with a diameter < 2 mm. Within the fine-root category, we separated roots into absorptive and transport roots. Absorptive roots are lower root orders, typically the first, second and third root orders (defined as the most distal root orders) and transport roots are higher order roots (all orders above the third order roots, Freschet & Roumet, 2017).

For each monolith, two subsamples of each root category (coarse, absorptive and transport roots, mean dry mass 2 g) were selected, spread into a transparent water-filled tray and scanned at 800 dpi (Epson Expression 1680, Canada). Images were analysed using the software Winrhizo Pro (Regent Instruments, Canada) to determine community-level root length (L_{com} , mm), mean root diameter (RD_{com} , mm), and root volume (V_{com} , cm^3). Each subsample was weighed after scanning to determine its fresh mass (RFM_{com} , g) and then oven-dried at 60°C for 72h to determine its dry mass (RDM_{com} , g). Remaining roots from the monolith were dried at 40°C for 72h and weighed to calculate their total dry biomass. The following morphological root traits were calculated at the whole plant community level (noted $\text{trait}_{\text{com}}$ hereafter): specific root length (SRL_{com} , m.g^{-1}) as the ratio between L_{com} and RDM_{com} ; and root dry matter content ($RDMC_{\text{com}}$, mg.g^{-1}) as the ratio between RDM_{com} and RFM_{com} . The root mass density (RMD_{com} , g.cm^{-3}) was calculated as the ratio between root mass_{com} (mass of scanned and non-scanned roots) and the soil rooting volume (half the monolith volume corrected for stone and very coarse root). Root length density (RLD_{com} , m.cm^{-3}) was the product of RMD_{com} and SRL_{com} .

Root chemical traits_{com} were determined on ground absorptive and transport roots (one replicate per monolith). The root nitrogen and carbon content (RNC_{com} and RCC_{com} mg.g^{-1}) was measured using an elemental analyser (CHN model EA 1108; Carlo Erba Instruments, Italy). The concentration of fibres (mg.g^{-1}), i.e. hydrosoluble compounds_{com}, hemicellulose_{com},

cellulose_{com} and *lignin_{com}* content was determined following the Van Soest method (Van Soest, 1963) using a fibre analyser (Fibersac 24; Ankom, Macedon, NJ, USA).

2.7. Soil physical and chemical properties

Soil physical and chemical properties were determined at the Laboratoire d'Analyses des sols (INRA, Arras, France) on each pooled soil sample harvested within each monolith. Soil texture was measured using the Robison's pipette and sieving techniques (NF X 31-107, Pansu & Gautheyrou, 2006). Soil particles were classified into three size fractions: clay (< 2 µm), silt (2-50 µm) and sand (50-2000 µm). Cationic exchange capacity (CEC, cmol.kg⁻¹) was determined in a cobalhexamin solution using the Matson method (NF X 31-130, Ciesielski *et al.*, 1997) and pH was measured in water (NF ISO 10390). Total soil organic carbon (SOC, g.kg⁻¹, NF ISO 10694) and total nitrogen content (TN, g kg⁻¹, NF ISO 13878) were determined by dry combustion (Girardin & Mariotti, 1991).

2.8. Structural (aggregate) stability

Structural, or aggregate stability was determined on soil samples taken from two depths (topsoil: 0-0.25 m and subsoil: 0.25-0.50 m, n = 140), using the fast wetting standard method (ISO/CD 10930, Le Bissonnais, 1996). This methodology is appropriate to compare the behaviour of a large range of soils during rapid wetting (mimicking heavy rain storms). Five grams of aggregates (3-5 mm) were gently immersed in 50 mL of deionized water for 10 minutes; water was then removed with a pipette and the soil material was transferred to a 50 µm sieve previously immersed in ethanol. The 50 µm sieve was gently moved five times to separate fragments < 50 µm. The > 50 µm fraction was collected, oven-dried and gently dry-sieved by hand on a column of six sieves: 2000, 1000, 500, 200, 100 and 50 µm. The mass percentage of each size fraction was calculated, and the aggregate stability was expressed by computation of the mean weight diameter (MWD) calculated as follows:

$$MWD = \sum d * \frac{m}{100} \quad \text{Eq. (2)}$$

where *d* is the mean diameter between two sieves (mm) and *m* the mass fraction (%) remaining in the sieve. Three tests were performed on each soil sample per monolith and soil depth (subdivided in three methodological replicates).

2.9. Statistical analysis

The six altitudinal levels showed quite clear disparities in soil coverage, species composition and climate. As a result, we chose to consider altitudinal levels as independent, and to process them as a qualitative variable. We tested the effect of the elevation level across and within keystone species, and the effect of the keystone species on soil processes, vegetation composition and masses, root traits_{com} and soil properties. Doing so we used weighted least square models (WLS). The great heteroskedasticity between altitudinal levels and keystone species was corrected using computer-assisted learning, adding to the ordinary least square models (OLS) the following weights (*W*):

$$W = \frac{1}{FVE^2} + \frac{1}{FVS^2} \quad \text{Eq. (3)}$$

Where *FVE* are the fitted values of the absolute residuals of the OLS on elevation, and *FVS* on keystone species. When the normality of residuals distribution was not met, variables were square-root or log transformed (see tables of tests). Effects were considered significant if *P* <

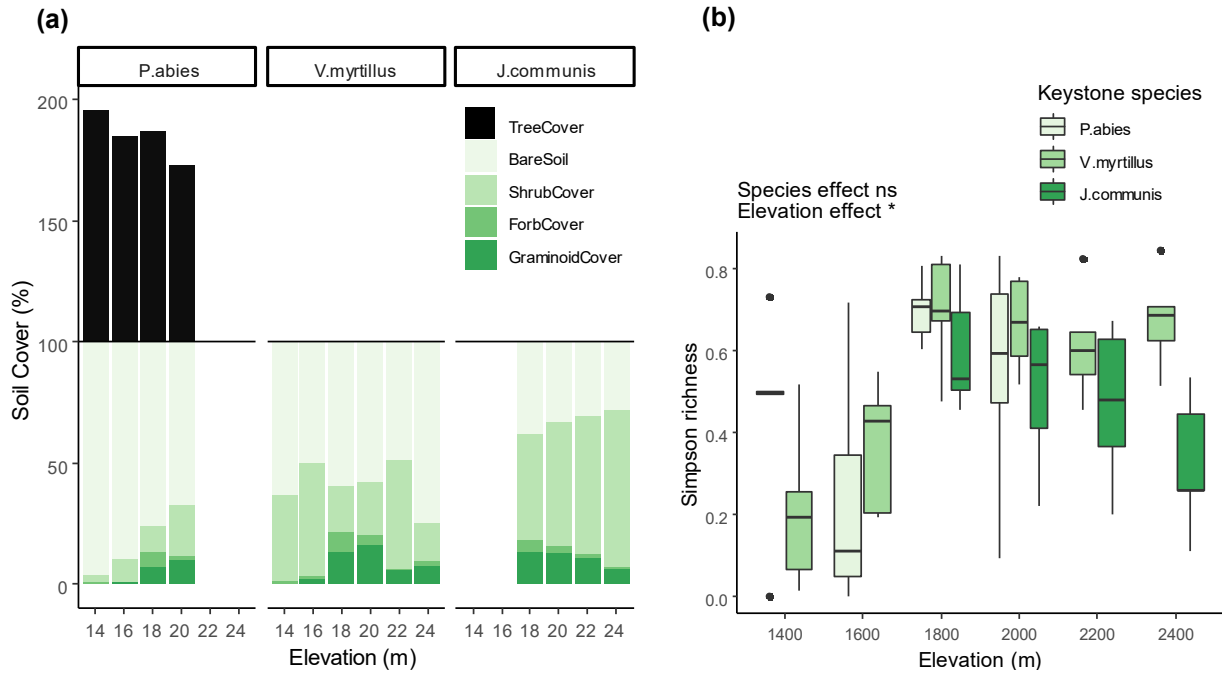


Figure 3: Differences in vegetation beneath keystone species and along the elevational gradient. (a) percentage of soil covered by bare soil, trees, shrubs, forbs and graminoids and (b) Simpson plant diversity index in the 1 x 1 m plots above the monoliths (Results of statistical WLS analyses are given in Table S6). In the boxplot, the lower edge of the box corresponds to the 25th percentile data point, while the top edge of the box corresponds to the 75th percentile data point. The line within the box represents the median and the black dots indicate outliers.

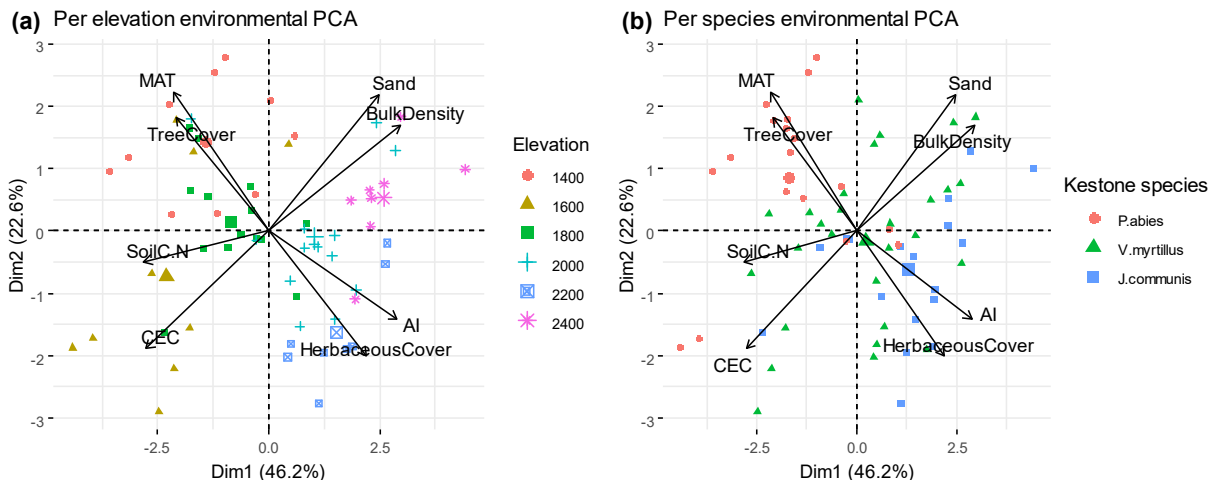


Figure 4: Biplot principal component analysis (PCA) of environmental variables. Monoliths are plotted according to their elevational level (a) and keystone species identity (b). Bigger points stand for centroids. For abbreviations, see Table S5.

0.05. Whenever significant effects were found, differences among means were explored using Tukey's honestly significant difference (HSD).

To characterize the gradient across altitudinal levels, we performed an environmental principal component analysis (PCA) including soil properties (CEC, soil C : N, bulk density and sand content), vegetation cover (tree and herbaceous cover) and modelled climatic data (MAT, AI). To have a finer characterization of the responses of roots traits_{com} and processes along environmental conditions we performed WLS analysis on the scores of the two first axes of the environmental PCA. PCA was performed on eight root traits (RD_{com}, SRL_{com}, RDMC_{com}, RNC_{com}, RCC_{com}, root cellulose_{com} and lignin_{com}) of absorptive and transport roots to visualize trait variation and covariation along elevation and across keystone species at the community level. There was strong collinearity between RDMC_{com} and RTD_{com}, thus we only used RDMC_{com} in this study. Prior to the PCA, variables were standardized using the zero-mean approach. Elevation and the keystone species identity were used as dummy variables. All statistical analyses were performed using R.3.4 software (R Core Team 2012; R Foundation for Statistical Computing, Vienna, AT) using FactoMineR package for PCA analysis (Lê *et al.*, 2008).

3. Results

3.1. Variation in environmental variables along the elevational gradient

Plant community composition changed significantly beneath keystone species and along the elevational gradient (Table S6, Figure 3). A greater percentage of bare soil ($72 \pm 10 \%$) and a lower percentage of shrub cover ($11 \pm 5 \%$) existed beneath *P. abies* compared to *V. myrtillus* and *J. communis* where bare soil was less ($39 \pm 7 \%$ and $27 \pm 8 \%$ resp., Figure 3a) and shrub cover was greater ($30 \pm 6\%$ and $54 \pm 11\%$ resp.). Bare soil decreased from $80 \pm 13 \%$ to $52 \pm 19 \%$ with elevation mainly due to the *P. abies* effect (Figure 3a). Trees were present only above the *P. abies* monoliths and decreased from $96 \pm 6 \%$ to $73 \pm 14 \%$ with elevation (Figure 3a, Table S6). Shrub cover increased with elevation from $19 \pm 13\%$ to $40 \pm 20\%$ while graminoid and forb covers were significantly greater near the treeline (1800 – 2000 m, Figure 3a). The Simpson plant diversity index did not vary in the communities growing beneath the three keystone species (Figure 3b), but changed significantly with elevation, with a minimum of 0.33 ± 16 at 1400 m and a maximum of 0.66 ± 0.06 at the treeline (1800 m), before decreasing slowly until 2400 m, where it was 0.50 ± 0.14 (Figure 3b).

Soil properties, did not change significantly among keystone species except CEC which was highest beneath *P. abies* ($23.3 \pm 5.4 \text{ cmol.kg}^{-1}$), and lower beneath *V. myrtillus* ($16.6 \pm 3.7 \text{ cmol.kg}^{-1}$) and *J. communis* ($15.4 \pm 3.8 \text{ cmol.kg}^{-1}$, Figure S11). Along the elevational gradient, a decrease in soil organic carbon (from $148.3 \pm 42.7 \text{ g.kg}^{-1}$ to $98.7 \pm 20.0 \text{ g.kg}^{-1}$, Figure S11d), CEC (from 15.4 ± 4.0 to $9.0 \pm 1.8 \text{ cmol.kg}^{-1}$, Figure S11g), soil C : N (from 20.2 ± 3.0 to 15.3 ± 1.0 , Figure S11f) with increasing altitude was observed. This was accompanied by an increase in sand content (from $250.2 \pm 33.1 \text{ g.kg}^{-1}$ to $432.8 \pm 58.9 \text{ g.kg}^{-1}$, Figure S11a), bulk density (from $0.39 \pm 0.13 \text{ g.cm}^{-3}$ to $0.71 \pm 0.09 \text{ g.cm}^{-3}$, Figure S11c) and soil pH (from 4.5 ± 0.2 to 5.1 ± 0.2 , Figure S11b) with elevation. Total nitrogen was maximum at 1600 m ($13.2 \pm 3.2 \text{ g.kg}^{-1}$) and minimum at 2400 m $6.4 \pm 1.1 \text{ g.kg}^{-1}$, Figure S11e).

Global characterization of the elevational gradient. Associations between climatic data, soil properties and vegetation cover were analysed using a PCA in order to characterize the elevational gradient (Figure 4, Table S7). The first axis explained 46 % of the total inertia and was driven by bulk density and aridity index on the positive side and by soil C : N and CEC on the negative side. The second axis explained 23 % of the total inertia and was driven by MAT,

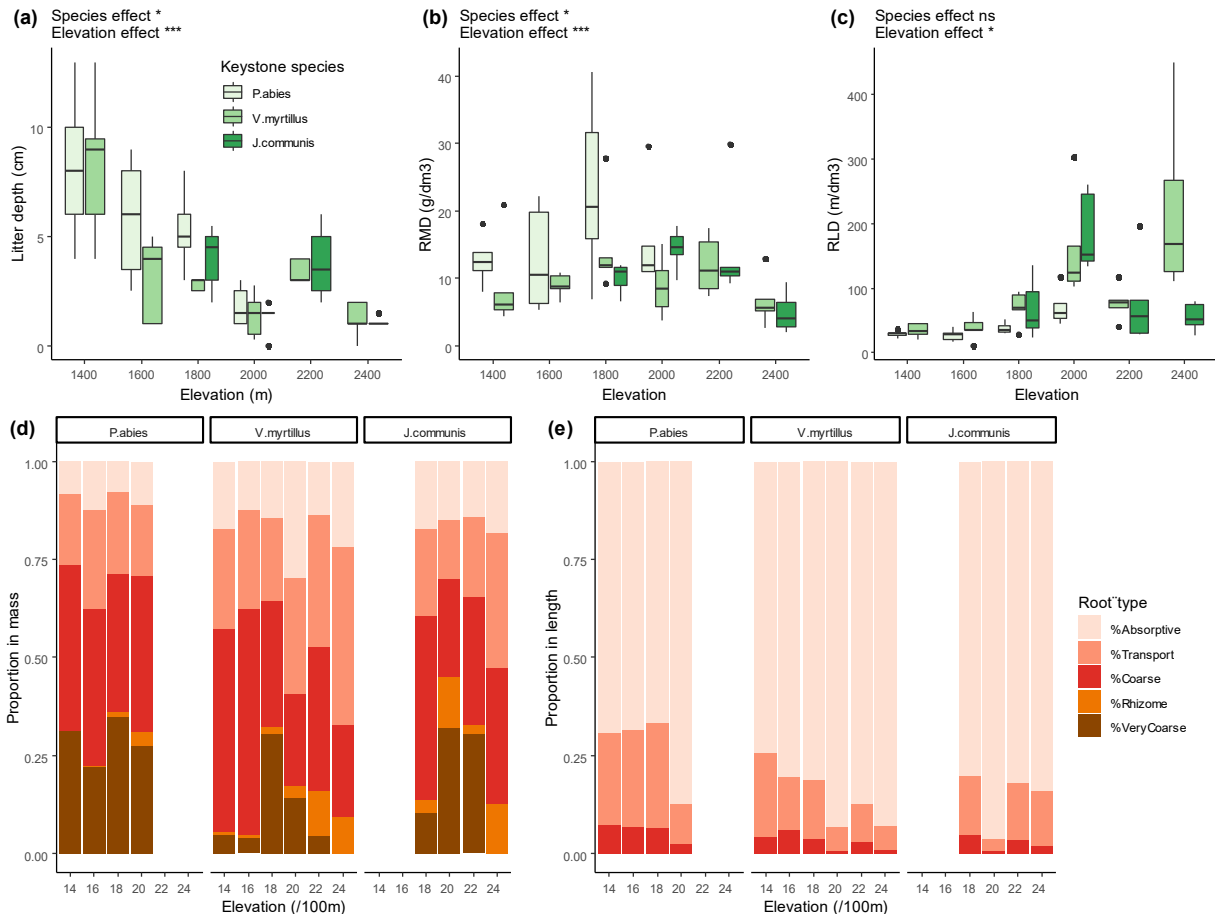


Figure 5: Difference in litter and roots beneath keystone species and along the elevational gradient. (a) litter root depth, (b) root mass density, (c) root length density, (d) proportion of root types in mass and (e) proportion of root types in length, excluding very coarse roots and rhizomes (Results of statistical WLS analyses are given in Table S6).

sand content and herbaceous cover. The above treeline monoliths (from 2000 to 2400 m) displayed positive scores on the first axis and below treeline monoliths (from 1400 to 1800 m) negative scores (Figure 4a). As *P. abies* grew at the lowest elevations, it benefited from a higher MAT with low herbaceous cover, at the opposite monoliths beneath *J. communis* were characterized by a greater aridity index and herbaceous cover while *V. myrtillus* showed intermediary values as it was present all along the gradient (Figure 4b). The scores of these two PCA axes were used to test the response of individual traits and soil processes to the global environment (see section 3.2. and 3.3.).

3.2. Influence of species and elevation on belowground components

3.2.1. Litter depth and root density

Litter depth was significantly different across keystone species: *P. abies* had the highest (5.3 ± 1.4 cm) compared to *V. myrtillus* (3.4 ± 1.0 cm) and *J. communis* (2.6 ± 0.8 cm, Figure 5a). Overall, litter depth decreased along the elevational gradient from 8.3 ± 2.0 to 12 ± 0.4 cm (Figure 5a).

The root mass density (RMD_{com}) had contrasted patterns beneath the keystone species due to differences in the proportion of root types. *P. abies* had the highest RMD_{com} (18.3 ± 5.8 g.dm⁻³) due to the lower proportion of absorptive (9.8 ± 3.0 %) and transport roots (20.7 ± 5.3 %, Table S6). RMD_{com} was lower in *V. myrtillus* (10.0 ± 1.9 g.dm⁻³) and *J. communis* (10.9 ± 2.7 g.dm⁻³, Figure 5b) due to the greater proportion of absorptive (18.9 ± 4.5 and 19.0 ± 6.2 % respectively) and transport roots (30.1 ± 3.9 and 23.0 ± 5.1 respectively, Figure 5b, Table S6). RMD_{com} decreased along the gradient from 15.4 ± 10.0 to 5.8 ± 2.1 g.dm⁻³ explained by an increase in the proportion of transport roots from 22.0 ± 6.6 to 44.9 ± 5.6 %, while coarse roots decreased from 47.0 ± 11.0 to 28.9 ± 13.5 %. Rhizome and very coarse root mass were different between elevational levels but were highly variable (Figure 5d, Table S6).

RLD_{com} did not vary globally beneath the keystone species even if a significant difference in the length of transport and coarse roots was observed. *P. abies* had the highest proportion in transport (21 ± 4 %) and coarse root length (6 ± 1 %) compared to *V. myrtillus* (transport: 11 ± 2 %, coarse: 3 ± 1 %) and *J. communis* (transport: 11 ± 4 %, coarse: 3 ± 1 %, Figure 5e, Table S6). RLD_{com} increased overall with elevation from $10,3 \pm 3.5$ to 35.0 ± 17.0 m.dm⁻³ (Figure 5c) explained by an increase in absorptive root proportion until 2200 m from 72 ± 4 % to 85 ± 7 % while the proportion of coarse roots decreased from 6 ± 1 % to 1 ± 1 % at 2400 m. Transport root proportion length was significantly different between altitudinal levels, but no clear pattern was evident with elevation (Figure 5e, Table S6).

3.2.2. Traits_{com} of absorptive and transport roots

Absorptive and transport root traits_{com} significantly changed along the gradient, sometimes in a non-linear pattern. Absorptive roots had higher RD_{com} beneath *P. abies* (0.30 ± 0.04 mm) compared to *V. myrtillus* (0.21 ± 0.03 mm) and *J. communis* (0.18 ± 0.03 mm, Figure 6a). The presence of *P. abies* resulted in a lower SRL_{com} in absorptive roots (23.8 ± 5.7 cm.g⁻¹) compared to *V. myrtillus* (53.0 ± 10.9 cm.g⁻¹) and *J. communis* (53.7 ± 11.2 cm.g⁻¹, Figure 6b). Overall SRL_{com} increased with elevation from 19.6 ± 2.4 to 85.9 ± 14.8 cm.g⁻¹ (Figure 6b), this is associated with by a decrease in RD_{com} of 53 % (Figure 6a) and a slight increase in $RDMC_{com}$ of 12 % (Figure 6c).

Transport root traits_{com} displayed no pattern beneath any of the keystone species (Figure 6). No difference in RD_{com} occurred in transport roots along elevation (Figure 6d). SRL_{com} varied

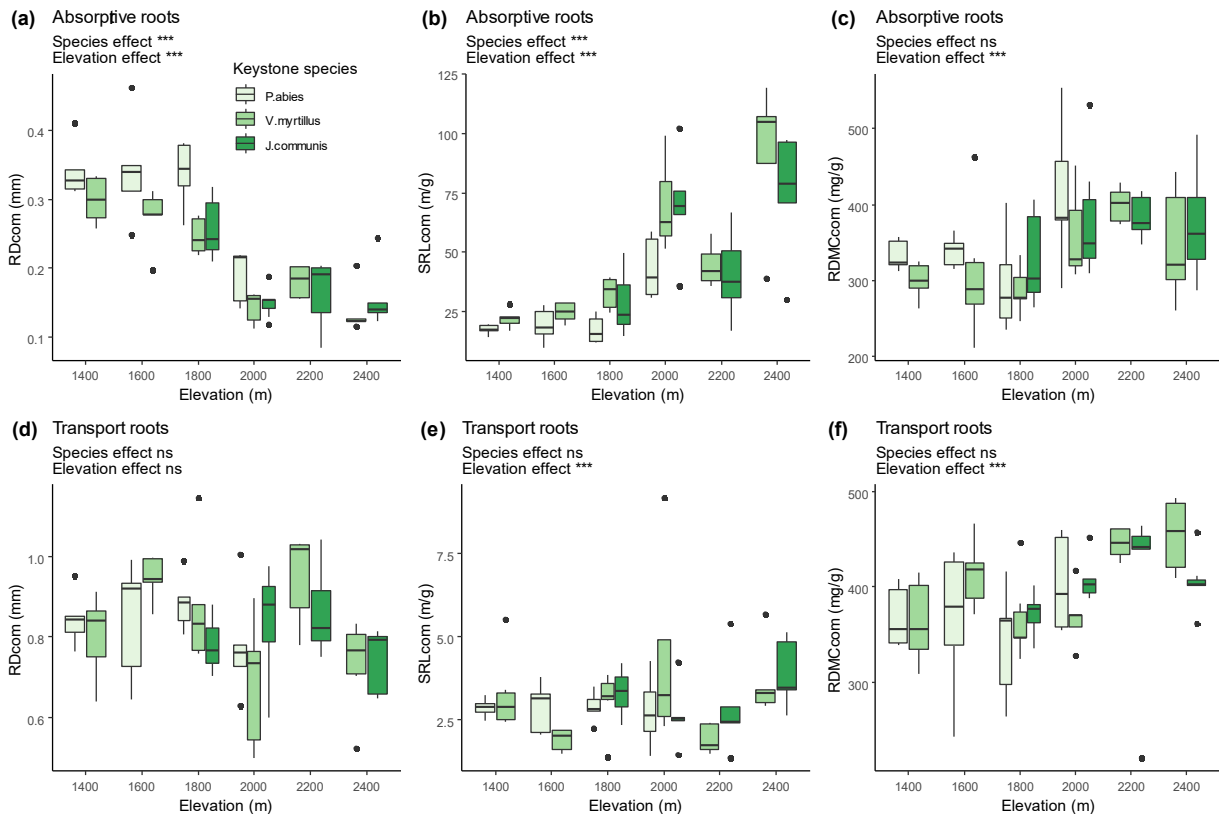


Figure 6: Differences in the community morphological root traits for both absorptive (a, b and c) and transport (d, e and f) roots beneath keystone species and along the elevational gradient. (a; d) community mean root diameter, (b;e) community specific root length, (c; f) community root dry mass content. Results of statistical WLS analyses are given in Table S6).

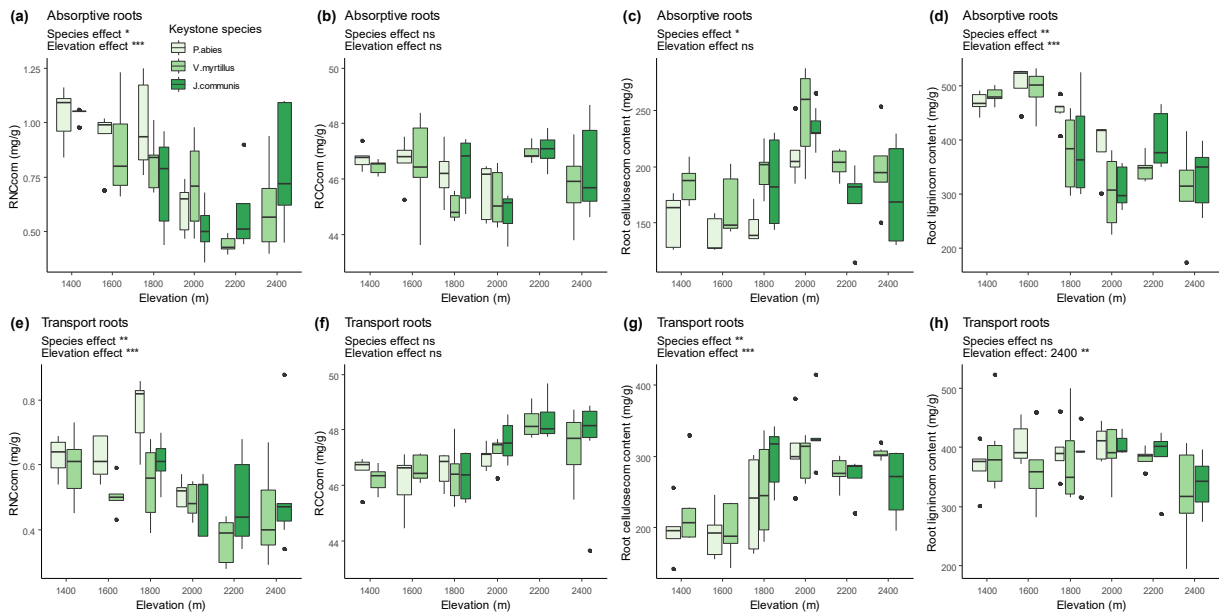


Figure 7: Differences in chemical root traits_{com} for both absorptive (a, b, c and d) and transport (e, f, g and h) roots beneath keystone species and along the elevational gradient. (a; e) community root nitrogen content, (b; f) community root carbon content, (c; g) community root cellulose content and (d; h) community root lignin content (Results of statistical WLS analyses are given in Table S6.).

between elevational levels, but showing no clear pattern. $RDMC_{com}$ increased significantly with elevation from $365 \pm 22 \text{ mg.g}^{-1}$ to $428 \pm 22 \text{ mg.g}^{-1}$ (Figure 6f).

Plant communities growing beneath *V. myrtillus* and *J. communis* possessed similar root chemical traits_{com} and usually differed from *P. abies*. Plant communities growing beneath *P. abies* had the highest RNC_{com} (absorptive: $0.88 \pm 0.09 \text{ mg.g}^{-1}$, transport: $0.63 \pm 0.05 \text{ mg.g}^{-1}$, Figure 7a, e), whereas the two other species were not significantly different from each other (Figure 7a, e). RNC_{com} decreased by 32 % in absorptive roots and 24 % in transport roots with increasing altitude (Figure 7a, e), whereas RCC_{com} was stable across keystone species and along the gradient for both absorptive and transport roots (Figure 7 b, f).

Plant communities structured by *P. abies* contained less root cellulose_{com} in absorptive roots ($163 \pm 15 \text{ mg.g}^{-1}$) than those beneath *V. myrtillus* ($198 \pm 13 \text{ mg.g}^{-1}$) and *J. communis* ($190 \pm 19 \text{ mg.g}^{-1}$, Figure 7c, g). However, plant communities beneath *P. abies* had higher lignin_{com} content in absorptive roots ($453 \pm 24 \text{ mg.g}^{-1}$) than those beneath *V. myrtillus* ($385 \pm 33 \text{ mg.g}^{-1}$) and *J. communis* ($362 \pm 31 \text{ mg.g}^{-1}$, Figure 7d), but did not differ with regard to transport roots (Figure 7g). Root cellulose_{com} reached its maximum at 2000 m for both absorptive ($232 \pm 15 \text{ mg.g}^{-1}$) and transport roots ($313 \pm 22 \text{ mg.g}^{-1}$, Figure 7c, g). Root lignin_{com} content decreased from 475 ± 11 to $319 \pm 45 \text{ mg.g}^{-1}$ for absorptive roots with increasing altitude, and did not differ between elevations in transport roots (Figure 7d, h).

3.2.3. Covariation of traits_{com} of absorptive and transport roots

Root functional space was visualized using principal component analysis (PCA, Figure 8). Regarding absorptive root traits_{com}, the first two axes of the PCA explained 76.3 % of the total inertia (Figure 8a, b; Table S8). The first axis was driven by lignin_{com} content, RD_{com} and RNC_{com} on the positive side and cellulose_{com} content and SRL_{com} at the negative side. The second axis was led by $RDMC_{com}$ and RCC_{com} on the positive scores. Concerning transport root traits_{com}, the two first axes explained 54.9 % of the total inertia (Figure 8c, d ; Table S8), the third axis explained an additional 16.9 %. The first axis opposed RD_{com} and $RDMC_{com}$ on the positive side and SRL_{com} on the negative side. The second axis was explained by RNC_{com} and lignin_{com} on the positive side, and $RDMC_{com}$ at the opposite. The third axis was mainly driven by lignin_{com}.

The biplots revealed that community root traits_{com} for both absorptive and transport roots varied along elevation, but poorly across keystone species (Figure 8a). Communities below the treeline (1400 to 1800 m) belonged to positive coordinates on the first axis for absorptive root traits_{com}, and to negative coordinates on the second axis for transport root traits_{com}. They were in both cases characterized by a greater content RD_{com} , RNC_{com} and lignin_{com} content. Root communities in above treeline plots (2000 to 2400 m) showed opposite patterns in the PCA. They were characterized by higher SRL_{com} , $RDMC_{com}$ and cellulose_{com} content.

3.2.4. Influence of environment on root traits_{com}

Bivariate relationships between each trait_{com} and environmental variables showed that absorptive root traits varied significantly with a large spectrum of variables. $RDMC_{com}$ only responded positively MAT and negatively with AI (Table 2) while other traits_{com} were explained by more environmental variables. RD_{com} was positively related to litter depth ($R^2 = 35\%$), MAT ($R^2=0.34$), tree cover ($R^2=30\%$), soil C : N ($R^2=21\%$) and negatively with AI ($R^2=60\%$), herbaceous cover ($R^2=24\%$) and bulk density ($R^2=21\%$, Table 2). SRL_{com} was positively correlated with AI ($R^2=49\%$), bulk density ($R^2=28\%$) and negatively with litter depth ($R^2=32\%$, Table 2). RNC_{com} was best explained by AI ($R^2=44\%$) and vegetation variables as tree cover ($R^2=12\%$) as positive relationships and herbaceous cover ($R^2=13\%$) as negative relationship. RCC_{com} , cellulose_{com}, lignin_{com} concentrations showed similar patterns of variation along almost all soil and vegetation properties. RCC_{com} varied positively with SOC ($R^2=19\%$)

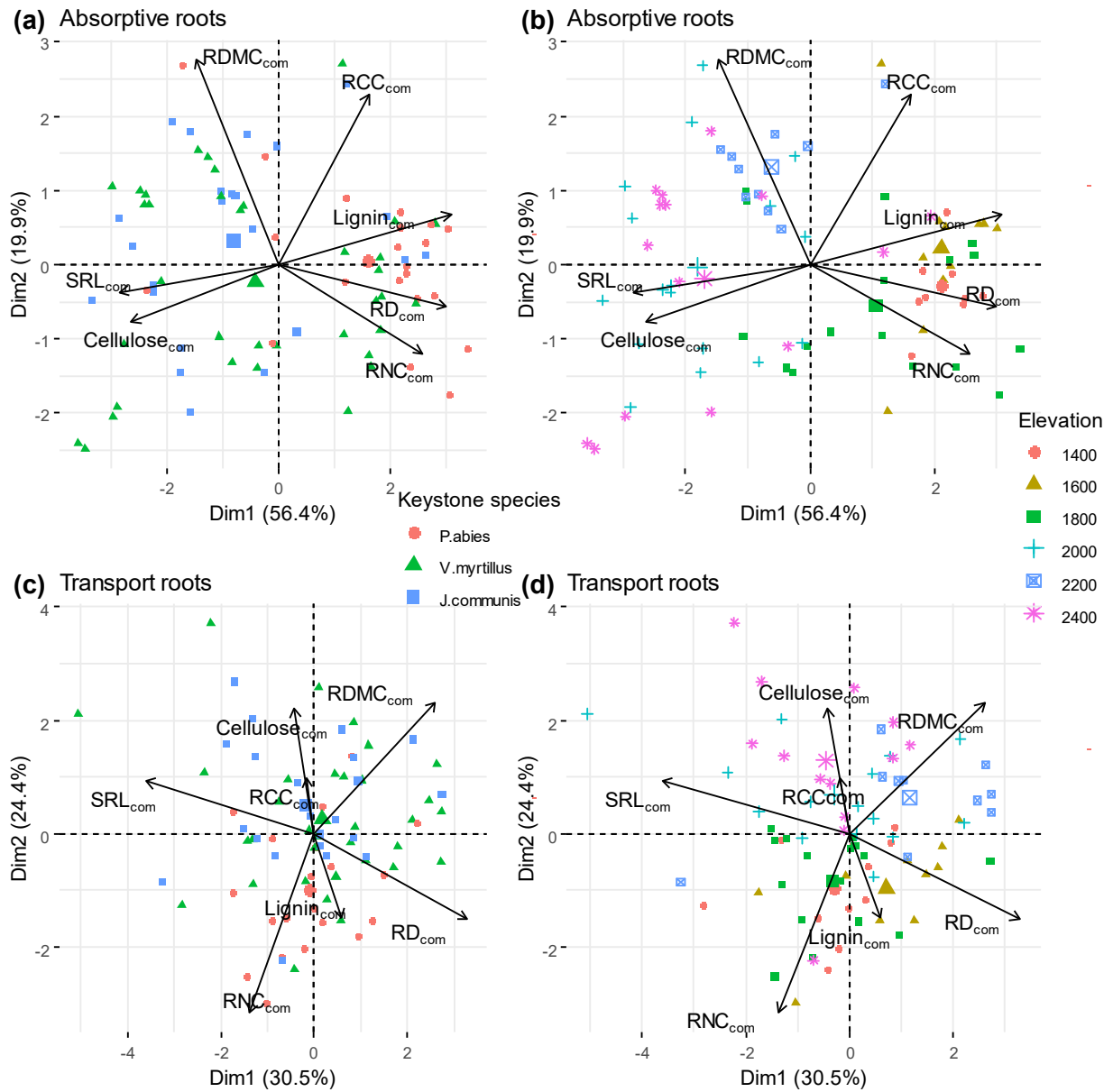


Figure 8: Biplot PCA for morphological and chemical root traits_{com} for both (a and b) absorptive roots and (c and d) transport roots. Data are plotted according to the species (a and c) and the elevation (b and d). Big points stand for centroids. For abbreviations, see Table S5.

and soil C : N ($R^2=18\%$), and negatively with pH ($R^2=23\%$, Table 2). Root cellulose_{com} was best explained by soil C : N ($R^2=25\%$) and SOC ($R^2=22\%$) as negative relationships and root lignin_{com} was best explained by AI ($R^2=42\%$) and bulk density ($R^2=32\%$) as positive relationships and MAT ($R^2=21\%$), soil C : N ($R^2=36\%$), litter depth ($R^2=32\%$) as negative ones (Table 2).

However, these simple bivariate analyses do not account for any potential interactions among environmental variables. Therefore, we tested whether root traits varied with PCA 1 axis which represented a gradient from soil monoliths with low CEC and C/N to those with high bulk density and aridity index, and with PCA 2 axis which represented a gradient from high MAT to high sandy soils and herbaceous cover. Traits of absorptive roots were all strongly related to PCA 1 axis (except RDMC_{com}) and only slightly correlated to PCA 2 axis (Table 2). Along the PCA 1 axis, RD_{com}, RNC_{com}, RCC_{com} and lignin_{com} concentration of absorptive roots decreased indicating that they are highest in monoliths with high CEC and C/N and lowest in monoliths with high bulk density (Figure S12). At the opposite SRL_{com} and cellulose_{com} concentration increased with PCA 1 while RDMC_{com} was stable (Figure S12). Along PCA 2, all traits were stable except for RD_{com} which increased and RCC_{com} which decreased (Figure S13). The same pattern was observed within each keystone species (Figure S12, Figure S13).

Transport root traits_{com} were not or poorly explained by environmental variables ($R^2<10\%$, Table 3). RNC_{com} only varied with climatic variables, positively with MAT ($R^2=29\%$) and negatively with AI ($R^2=26\%$). Cellulose_{com} concentration was best explained by AI ($R^2=26\%$) as positive relationship and by litter depth ($R^2=20\%$) and soil C : N ($R^2=16\%$) as negative ones (Table 3). Overall, RDMC_{com} and cellulose_{com} concentration increased along PCA 1, RNC_{com} decreased while the other traits_{com} (RD_{com}, SRL_{com}, RCC_{com} and lignin_{com}) did not vary significantly (Figure S14). Along PCA 2, SRL_{com} showed a positive relationship and RD_{com}, RDMC_{com} and RCC_{com} decreased (Figure S15).

3.3. Influence of species and elevation on soil processes

3.3.1. Soil processes

Soil mean weight aggregate diameters (MWD) were all >2 mm (ranging from 2.13 to 3.45 mm) indicating that aggregates are very stable (according to the classification by Le Bissonnais, 1996). We found no significant effect of the species on either the sub- or top-soil MWD (Figure 9a, b). Overall, topsoil aggregate stability was significantly lower at 2400 m (Figure 9a), due to the 11 % decrease observed beneath *J. communis* (Figure 9a). A global decrease in the subsoil MWD from 3.13 ± 0.06 mm to 2.51 ± 0.33 mm was observed (Figure 9b) mainly due to the 26 % decrease observed beneath *V. myrtillus* (Figure 9b).

Hydraulic conductivity (*Kfs*) ranged from 1.0 to 37.7 $\text{cm}\cdot\text{h}^{-1}$ and was greater beneath *P. abies* (12.7 ± 4.0 $\text{cm}\cdot\text{h}^{-1}$) than the two other species (*V. myrtillus*: 7.0 ± 1.9 $\text{cm}\cdot\text{h}^{-1}$ and *J. communis*: 7.8 ± 3.2 $\text{cm}\cdot\text{h}^{-1}$, Figure 9c). Overall, the infiltration rate decreased significantly along elevation from 12.1 ± 3.9 $\text{cm}\cdot\text{h}^{-1}$ to 6.9 ± 4.0 $\text{cm}\cdot\text{h}^{-1}$, due mainly to a 50 % decrease in *Kfs* beneath *V. myrtillus* (Figure 9c, Table S6).

3.3.2. Influence of environment on soil processes

MWD in the topsoil was negatively correlated with bulk density ($R^2=26\%$) and sand content ($R^2=14$) and positively with litter depth ($R^2=16\%$) and RMD_{com} ($R^2=14\%$, Table 4). To a lesser extent, it was correlated negatively with mass proportion in absorptive ($R^2=9\%$) and transport roots ($R^2=11\%$) and positively with SOC ($R^2=10\%$, Table 4). None of the root morphological and chemical traits had a significant impact on MWD in the topsoil (Table 4).

Table 2: Linear models between absorptive root traits and environmental variables. Levels of significance: * is $p < 0.05$, ** is $p < 0.01$, *** is $p < 0.001$ and ns is not significant.

		Absorptive roots													
		RD		SRL		RDMC		RNC		RCC		Cellulose		Lignin	
		p	R ²	p	R ²	P	R ²	p	R ²	p	R ²	p	R ²	p	R ²
Vegetation	Tree cover (sqrt)	***	0.30	***	0.27	Ns		**	0.12	ns		**	0.14	***	0.18
	Bare soil (sqrt)	*	0.09	*	0.05	*	0.05	ns		*	0.08	ns		ns	
	Herbaceous cover (sqrt)	***	0.24	*	0.07	ns		**	0.13	ns		**	0.10	**	0.12
	Litter depth (sqrt)	***	0.35	***	0.32	ns		ns		**	0.12	***	0.21	***	0.32
Climate	MAT	***	0.34	***	0.23	***	0.18	***	0.33	ns		***	0.14	***	0.21
	AI	***	0.60	***	0.49	***	0.22	***	0.44	ns		***	0.19	***	0.42
Soil properties	Sand (log)	***	0.13	***	0.14	ns		ns		*	0.08	**	0.10	***	0.18
	pH (log)	***	0.18	***	0.23	ns		*	0.06	***	0.23	**	0.12	***	0.26
	Bulk density (sqrt)	***	0.21	***	0.28	ns		*	0.06	**	0.10	***	0.15	***	0.32
	SOC (log)	**	0.11	***	0.14	ns		*	0.08	**	0.19	***	0.22	***	0.29
	Soil C : N	***	0.22	***	0.28	ns		*	0.08	***	0.18	***	0.25	***	0.36
	CEC (log)	**	0.13	***	0.14	ns		*	0.07	*	0.09	***	0.15	***	0.29
Env	PCA 1	***	0.48	***	0.23	*	0.08	***	0.28	**	0.16	***	0.34	***	0.53
	PCA 2	*	0.06	ns		ns		ns		*	0.07	ns		ns	

Table 3: Linear models between transport root traits and environmental variables. Levels of significance are: * is $p < 0.05$, ** is $p < 0.01$, *** is $p < 0.001$ and ns is not significant.

		Transport roots													
		RD		SRL		RDMC		RNC		RCC		Cellulose		Lignin	
		p	R ²	p	R ²	p	R ²	p	R ²	p	R ²	P	R ²	p	R ²
Vegetation	Tree cover (sqrt)	ns		ns		*	0.07	***	0.21	ns		**	0.12	ns	
	Bare soil (sqrt)	ns		ns		ns		ns		ns		Ns		ns	
	Herbaceous cover (sqrt)	ns		ns		ns		*	0.08	*	0.08	**	0.14	ns	
	Litter depth (sqrt)	ns		ns		*	0.08	***	0.15	ns		***	0.20	ns	
Climate	MAT	ns		ns		**	0.11	***	0.29	ns		*	0.08	ns	
	AI	ns		ns		**	0.14	***	0.26	ns		***	0.27	ns	
Soil properties	Sand (log)	*	0.06	ns		*	0.08	ns		ns		**	0.01	ns	
	pH (log)			*	0.07	ns		ns		ns		**	0.14	ns	
	Bulk density (sqrt)	**	0.12	**	0.10	ns		*	0.06	ns		**	0.10	ns	
	SOC (log)	**	0.09	*	0.07	ns		ns		ns		**	0.12	ns	
	Soil C : N	ns		*	0.08	ns		ns		ns		***	0.16	ns	
	CEC (log)	ns		ns		ns		*	0.09	ns		.	0.05	ns	
Env	PCA 1	ns		ns		**	0.11	***	0.20	ns		***	0.20	ns	
	PCA 2	*	0.07	**	0.11	*	0.08	ns		**	0.11	Ns		ns	

In the subsoil, variation in MWD was positively related to litter depth ($R^2=24\%$) and SOC ($R^2=12\%$) and negatively related to bulk density ($R^2=24\%$, Table 4). These variables were accompanied by in a positive relationship with absorptive and transport RD_{com} , RNC_{com} and root lignin $_{com}$ content and negative with SRL_{com} (R^2 around 10% each, Table 4). It was also positively correlated with the proportion of coarse root mass ($R^2=12\%$) and negatively with the proportion in absorptive ($R^2 = 10\%$) and transport root mass ($R^2=7\%$, Table 4).

Kfs was significantly related to CEC ($R^2=22\%$), soil C.N ($R^2=13\%$) and SOC ($R^2=12\%$) in a positive way and with bulk density in a negative way ($R^2=10\%$, Table 4). The mass proportion of very coarse roots also explained positively Kfs ($R^2=11\%$, Table 4). Among root traits, Kfs was positively explained by RNC_{com} and Lignin $_{com}$ concentration of absorptive roots ($R^2=8$ and 10%, Table 4). Overall top- and sub- soil MWD and Kfs decreased along PCA 1 (Figure S16). Only topsoil MWD decreased significantly along PCA 2 (Figure S17).

4. Discussion

We demonstrated at the community level that plant root traits were modified along the elevational gradient. At higher altitudes with a cooler, wetter climate and less fertile soil, roots possessed morphological traits that were better able to exploit soil in the shorter growing season. These changes in root traits were reflected to a certain extent in the soil physical properties, affecting aggregate stability but not hydraulic conductivity, that was more related to litter thickness. The presence of keystone species in a plant community had little effect on soil properties, but as plant diversity was very high at all sites, the effects of individual species on soil processes may have been masked.

4.1. The keystone species impacted vegetation but not soil properties

Plants are known to have an influence on soil properties and litter production through their traits (Wardle *et al.*, 2004 ; Sundqvist *et al.*, 2012 ; Freschet *et al.*, 2018). Our three keystone species shaped different soil cover, root composition and fine-root traits (Table S6) but had a poor influence on soil properties and soil processes (Table 4). As we selected three contrasted growth form and deciduous status, we expected the structuring species influence to be contrasted between the three of them. In the end, we mainly observed a difference in root composition between the tall evergreen tree *P. abies* and the two other shrub species, while we expected the evergreen shrub *J. communis* to shape different plant communities compared to the deciduous shrub *V. myrtillus*. As *P. abies* high canopy intercepted a great part of the light and induced a marked shade, the growth of other species was therefore limited as indicated by the proportion of bare soil, which represented 70 to 95% of the soil cover beneath *P. abies* (Figure 3). The roots beneath *P. abies* thus belong mostly to *P. abies*; they are coarse, rich in C and lignin, three traits characteristic of tree species that favour root longevity and anchorage (Figure 3; Freschet *et al.* 2017). At the opposite, *V. myrtillus* and *J. communis* grew in full-lighted open areas, promoting the growth of herbaceous species. The roots beneath *J. communis* and *V. myrtillus* belongs to these shrubs, which have thinner roots than tree species, but also to herbaceous species, which have very fine root with high SRL and cellulose content but lower tissue density as compared to woody species (Figure 3; 12; Freschet *et al.* 2017; Ma *et al.* 2018).

4.2. Influence of elevation on roots

Our results showed that plants from higher elevations produce similar root biomass but a greater proportion of fine vs coarse roots, confirming the results reported both at the species by Körner & Renhardt, (1987) and Zadworny *et al.* (2016) and the community level by Blume-Werry *et al.*, (2018) along elevation. These absorptive roots are characterized by lower diameter and higher SRL, two traits that increase the soil exploration efficiency in the shorter

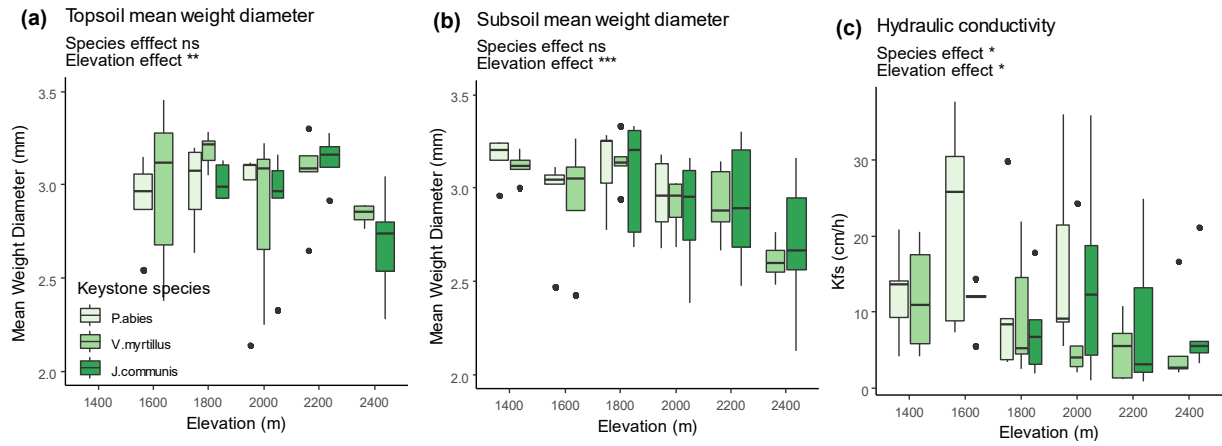


Figure 9: Differences in soil processes beneath keystone species and along the elevational gradient. Mean weight diameter of soil macro-aggregates collected (a) in the topsoil and (b) in the subsoil and (c) soil hydraulic conductivity (Results of statistical WLS analyses are given in Table S6).

growing season. They can also reflect a possible adaptation to a lower occurrence of mycorrhizal interactions at high elevation. Our data demonstrated that MAT and AI are the main driver of variation in RD and SRL. We observed a gradual increase in RD and a decline in SRL with increasing MAT, as reported by Freschet *et al.* (2017) in a meta-analysis on more than 300 species worldwide. However, an opposite pattern has been reported by Zadworny *et al.*, (2017) in a study examining intraspecific variation of root traits of *Pinus sylvestris* across a strong temperature and latitudinal gradient in Europe. Variation in RD, SRL and lignin concentration are correlated with variation in tree and herbaceous cover (Table 3). This suggest that the shift in the root community traits between low and high elevation is also explained by the replacement of plants from forest communities by shrub and herbaceous species. We hence had thicker, more lignified roots belonging to trees below the treeline plots (1400 – 1800 m) to finer, cellulose and nitrogen rich roots belonging to herbaceous species above the treeline (2000 – 2400 m, Figure 6). Root nitrogen content decrease along the elevational gradient, certainly as a consequence of lower nutrient availability at high elevation (Li *et al.*, 2019) or/and as a consequence of the dominance of graminoids at high elevation which have low RNC as compared to tree species (Freschet *et al.* 2017).

Plant communities from high elevations produced absorptive roots with a higher tissue density (high RDMC) than plant communities from low elevations, even though tree species which have a high RDMC are more abundant at low elevations. This result suggests, in agreement with our hypothesis, that to cope with extreme variations in climate and greater disturbances from e.g. snowmelt and rain storms at high elevations, plant produce absorptive and transport roots with a high tissue density in order to increase their persistence. As the production of roots during the short growing season is expensive for a plant, longer lived, more persistent roots would be a careful strategy at high elevations. Higher tissue density is also associated with higher mechanical strength of roots (Pohl *et al.*, 2011 ; Mao *et al.*, 2018), which enable plants to withstand uprooting and to remain anchored in the soil, e.g. during grazing, intense rainfall (Ennos & Pellerin, 2000) or at times of soil movement (Jonasson & Callaghan, 1992), perturbations that are frequent at high elevation.

4.3. Variation in erodibility and infiltration was mainly explained by the physical environment and to a lesser extent by vegetation

Aggregate stability was significantly related to SOC, soil texture and porosity, as also found by e.g., Erktan *et al.*, (2016) and Le Bissonnais *et al.*, (2018). Stability was also higher when the litter layer was deep, probably due to the high input of C into soil from the litter. Carbon increases aggregate stability when present in extracellular polymeric substances, including polysaccharides from root and fungal exudates, that act as an organic binding agent and "glue" soil particles together. However, as aggregate stability was high, corresponding to the very stable class of aggregates (Le Bissonnais, 1996), it was not influenced by the presence of individual keystone species and was poorly related to vegetation cover and root traits. Our data confirmed though the fine-root traits effects explored by Erktan *et al.*, (2016) which found that thicker roots and lower specific root length promoted aggregate stability. High root mass density favoured aggregate stability, probably through the physical enmeshing of soil particles and introduction of labile C into soil from root exudation stimulating thus the production of microbial metabolites involved in stability (Tisdall and Oates 1982, Erktan *et al.*, 2016 ; Le Bissonnais *et al.*, 2018). Surprisingly, the proportion of fine roots was negatively correlated to stability, that may be due to the high variability observed in the data, as the R² was very low. Also, plant diversity in our sampling was very high, with up to 120 species present at the monolith sites. Previous studies have shown that aggregate stability is positively influenced by a greater species diversity, but beyond a given number of species (>16), the effects on aggregate stability are limited (Pérès *et al.*, 2013 ; Berendse *et al.*, 2015 ; Gould *et al.*, 2016).

Table 4 : Linear models between soil processes and environmental variables and roots. Levels of significance are: * is $p < 0.05$, ** is $p < 0.01$, *** is $p < 0.001$ and ns is not significant.

		MWD top (sqrt)		MWD sub (sqrt)		Kfs (log)	
		p	R ²	p	R ²	p	R ²
Vegetation	Tree cover (sqrt)	ns		ns		*	0.09
	Bare soil (sqrt)	ns		*	0.05	*	0.06
	Herbaceous cover	ns		ns		*	0.07
Dry mass	Litter depth (sqrt)	**	0.16	***	0.24	**	0.16
	Root Mass Density (sqrt)	**	0.14	*	0.09	ns	
	% Mass Ab (sqrt)	*	0.09	**	0.10	*	0.08
	% Mass Tp (sqrt)	**	0.11	*	0.07	*	0.08
	% Mass Co (sqrt)	ns		**	0.12	ns	
	% Mass Rh (sqrt)	ns		ns		ns	
	% Mass vCo (sqrt)	ns		ns		**	0.11
	Root Length Density (sqrt)	ns		ns		ns	
	% Length Ab (sqrt)	ns		ns		ns	
	% Length Tp (sqrt)	ns		*	0.06	*	0.07
	% Length Co (sqrt)	ns		**	0.12	ns	
	Absorptive roots traits	Ab RD	ns		**	0.11	*
Ab SRL (log)		ns		*	0.08	ns	
Ab RDMC (log)		ns		ns		ns	
Ab RNC (sqrt)		ns		*	0.09	X	
Ab RCC (log)		ns		ns		X	
Ab Cellulose (log)		ns		ns		X	
Ab Lignin (log)		ns		**	0.10	X	
Transport root traits	Tp RD (sqrt)	ns		**	0.11	ns	
	Tp SRL (log)	ns		ns		ns	
	Tp RDMC (log)	ns		*	0.05	ns	
	Tp RNC (sqrt)	ns		*	0.10	X	
	Tp RCC (log)	ns		ns		X	
	Tp Cellulose (log)	ns		ns		X	
	Tp Lignin (log)	ns		**	0.10	X	
Soil	Sand (log)	**	0.14	**	0.09	ns	
	Bulk density (sqrt)	***	0.26	***	0.24	**	0.10
	SOC (log)	*	0.10	**	0.12	**	0.12
	Soil C : N (log)	ns		ns		**	0.13
Env	PCA 1	*	0.08	**	0.15	***	0.25
	PCA 2	***	0.22	ns		ns	

The reasons for this limit to aggregate stability maybe because a wide variety of root traits are present in diverse species mixtures, suggesting that all possible mechanisms for improving stability, such as C input and physical enmeshing of soil particles, can be accomplished by a fairly small number of plant species with diverse root systems. Therefore, taking into account a hierarchical approach, considering the effects of individual species and selected species mixtures would better elucidate the influence of keystone species on soil processes. Also, values of trait diversity, rather than trait means, could explain certain effects on soil properties observed at the community level.

As with aggregate stability, water infiltration into soil was related soil bulk density and SOC, as also found in previous studies (Lado *et al.*, 2004 ; Hiraoka & Onda, 2012). However, we found no effect of texture on infiltration, unlike results from similar studies (Hiraoka & Onda, 2012 ; Marín-Castro *et al.*, 2017). Litter depth had the greatest positive effect on infiltration, followed by the proportion of coarse roots present in soil, although variability in the data was high. Marín-Castro *et al.* (2017) also found that litter depth was the main factor affecting infiltration in a coffee plantation, and suggested that the litter layer could maintain a local microclimate (humidity and temperature) that indirectly keeps the soil pores active, facilitating water conduction. The positive effect of coarse roots on infiltration is because they create preferential streams for water flow in soil (Ghestem *et al.*, 2011) though Nespoulous *et al.* (2019) found a greater effect of fine roots on water infiltration, in mixed forests on Ferralsols. Therefore, soil type likely influences water flux through preferential channels and pores, but studies are limited and so mechanisms are poorly understood.

5. Conclusion

We showed that at the community level, plant root traits were modified along an elevational gradient. At higher altitudes with a cooler, wetter climate, plant communities had strong specific adaptations to cope with the cold temperatures that limit mineralization rates and nutrient availability. These adaptations include strategies for better acquiring belowground resources in the short growing season, through an increased production of roots with high absorptive capacity that are characterized by small diameters and high SRL. Roots also demonstrated strategies for increasing persistence through the production of thicker roots with greater RTD and more structural and defence compounds. The root trait adaptation to elevation is likely a compromise between specialisation in resource capture or increased investment in tissue protection. Changes in root traits were reflected to a certain extent in the soil physical properties, affecting aggregate stability but not hydraulic conductivity (except for very thick roots that created preferential flow channels). These soil properties were more influenced by soil carbon content and the thickness of the litter layer, that altered the local soil microclimate and chemical properties. The presence of keystone species in a plant community had little effect on soil properties but, as plant diversity was very high at all sites, the effects of individual species on soil processes may have been masked. Future work should comprise elements not taken into account in this study, such as the activity and diversity of soil fauna and micro-organisms, that can also alter soil properties, and play an important role in the functioning of plant communities.

6. Supplementary materials

Table S5: Abbreviations used in the text.

Variable	Meaning	Variable	Meaning
MWD top	Mean Weight Diameter topsoil	RCC	Root Carbon Content
MWD sub	Mean Weight Diameter subsoil	SOC	Soil Organic Carbon
Kfs	Hydraulic conductivity	CEC	Cationic Exchange Capacity
RD	Root Diameter	MAT	Mean Annual Temperature
SRL	Specific Root Length	MAP	Mean Annual Precipitation
RDMC	Root Dry Matter Content	ETP	Evapotranspiration
RNC	Root Nitrogen Content	AI	Aridity Index
		GSL	Growing Season Length

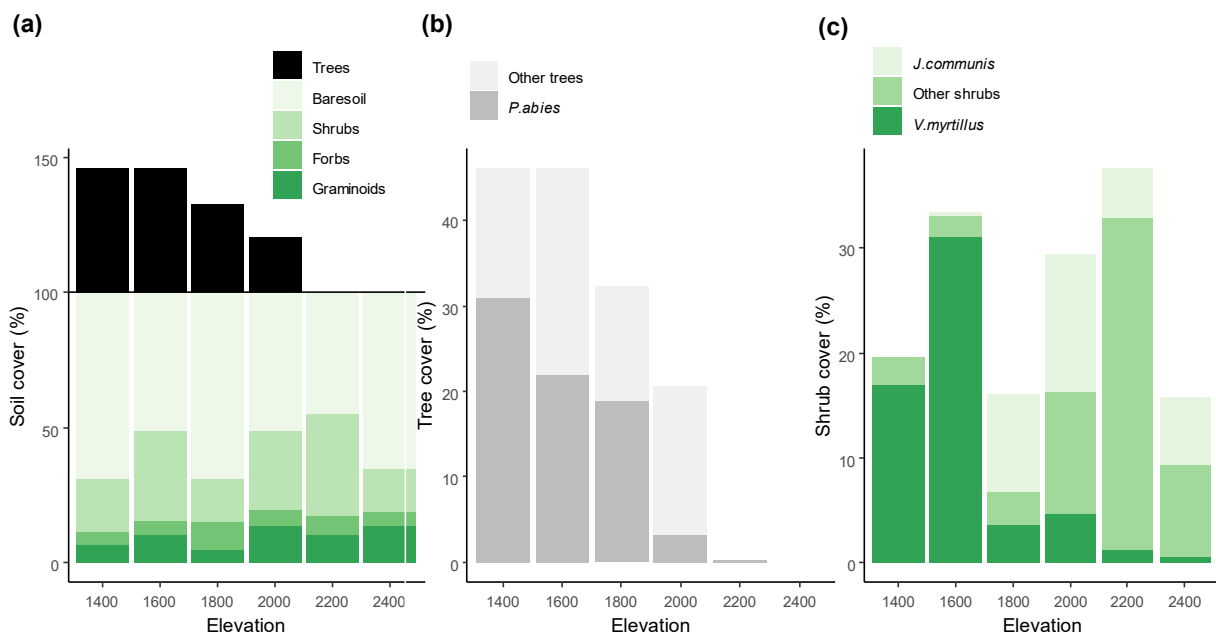


Figure S10: Differences in soil cover in plots (20 x 20 m) along the elevational gradient: (a) percentage cover of bare soil and vegetation per plant growth forms (trees, shrubs, forbs and graminoids). (b) Percentage cover of *P. abies* (single tree keystone species) compared to cover from other tree species and (c) Percentage cover of *V. myrtillus* and *J. communis* (two shrub keystone species) compared to cover from other shrub species.

Table S6: Linear weighted models between variables and elevation among and within keystone species. Levels of significance are: * is $p < 0.05$, ** is $p < 0.01$, *** is $p < 0.001$ and ns is not significant.

		Species effect		Elevation effect		Elevation effect					
						<i>P. abies</i>		<i>V. myrtillus</i>		<i>J. communis</i>	
		p	R ²	p	R ²	p	R ²	p	R ²	p	R ²
Vegetation	Tree cover (sqrt)	****		****		*	0.41	ns		ns	
	Bare soil (sqrt)	***	0.50	*	0.17	**	0.82	ns		ns	
	Shrub cover (sqrt)	****	0.48	**	0.21	ns		***	0.60	ns	
	Forb cover (sqrt)	ns		***	0.28	ns		ns		ns	
	Graminoid cover (sqrt)	****	0.29	****	0.51	**	0.58	****	0.70	ns	
	Simpson (sqrt)	ns		***	0.32	*	0.44	***	0.63	ns	
Root density	Litter depth (sqrt)	*		****	0.54	***	0.68	***	0.60	*	0.40
	Root Mass Density (sqrt)	*	0.10	***	0.32	ns		ns		***	0.64
	% Mass Ab (sqrt)	**	0.15	ns		ns		ns		ns	
	% Mass Tp (sqrt)	**	0.13	**	0.23	ns		***	0.70	ns	
	% Mass Co (sqrt)	ns		*	0.18	ns		***	0.56	ns	
	% Mass Rh (sqrt)	***	0.20	***	0.32	ns		*	0.39	ns	
	% Mass vCo (sqrt)	ns		***	0.44	ns		***	0.56	**	0.50
	Root Length Density (sqrt)	ns		*	0.06	ns		ns		ns	
	% Length Ab (sqrt)	ns		***	0.27	***	0.82	***	0.98	ns	
	% Length Tp (sqrt)	***	0.21	***	0.45	***	0.83	***	0.49	***	0.55
% Length Co (sqrt)	**	0.15	***	0.51	***	0.67	***	0.70	ns		
Morphological traits	Ab RD	****	0.27	****	0.73	ns		**	0.53	ns	
	Ab SRL (log)	***	0.23	***	0.60	***	0.49	***	0.70	***	0.50
	Ab RDMC (log)	*	0.05	****	0.26	*	0.25	***	0.35	ns	
	Tp RD (sqrt)	ns		ns		ns		**	0.54	ns	
	Tp SRL (log)	ns		***	0.16	ns		**	0.52	*	0.22
	Tp RDMC (log)	*	0.05	***	0.20	ns		***	0.61	*	0.24
Chemical trait	Ab RNC (sqrt)	**	0.18	****	0.65	***	0.67	****	0.97	*	0.41
	Ab RCC (log)	ns		ns		ns		****	0.73	**	0.54
	Ab Cellulose (log)	**	0.18	****	0.46	***	0.67	**	0.50	**	0.54
	Ab Lignin (log)	***	0.21	****	0.64	**	0.52	****	0.82	*	0.40
	Tp RNC (sqrt)	**	0.16	****	0.41	***	0.66	**	0.52	.	
	Tp RCC (log)	ns		ns		ns		ns		**	0.50
	Tp Cellulose (log)	**	0.14	****	0.52	**	0.52	****	0.58	ns	
Tp Lignin (log)	ns		*	0.19	ns		ns		ns		
Processes	MWD top (sqrt)	ns		**	0.22	ns		ns		*	0.40
	MWD sub (sqrt)	ns		***	0.28	ns		*	0.38	ns	
	Kfs (log)	*		*	0.17	ns		*	0.36	ns	
Soil properties	Sand (log)	ns		****	0.43	ns		****	0.63	*	0.42
	pH (log)	ns		****	0.46	ns		****	0.68	*	0.39
	Bulk density (sqrt)	ns		****	0.56	**	0.56	****	0.66	***	0.64
	SOC (log)	ns		****	0.35	ns		ns		ns	
	Soil N	ns		***	0.36	*	0.39	*	0.40	ns	
	Soil C : N	ns		***	0.49	*	0.38	***	0.75	***	0.60
	CEC (log)	*	0.17	****	0.44	ns		*	0.39	*	0.38

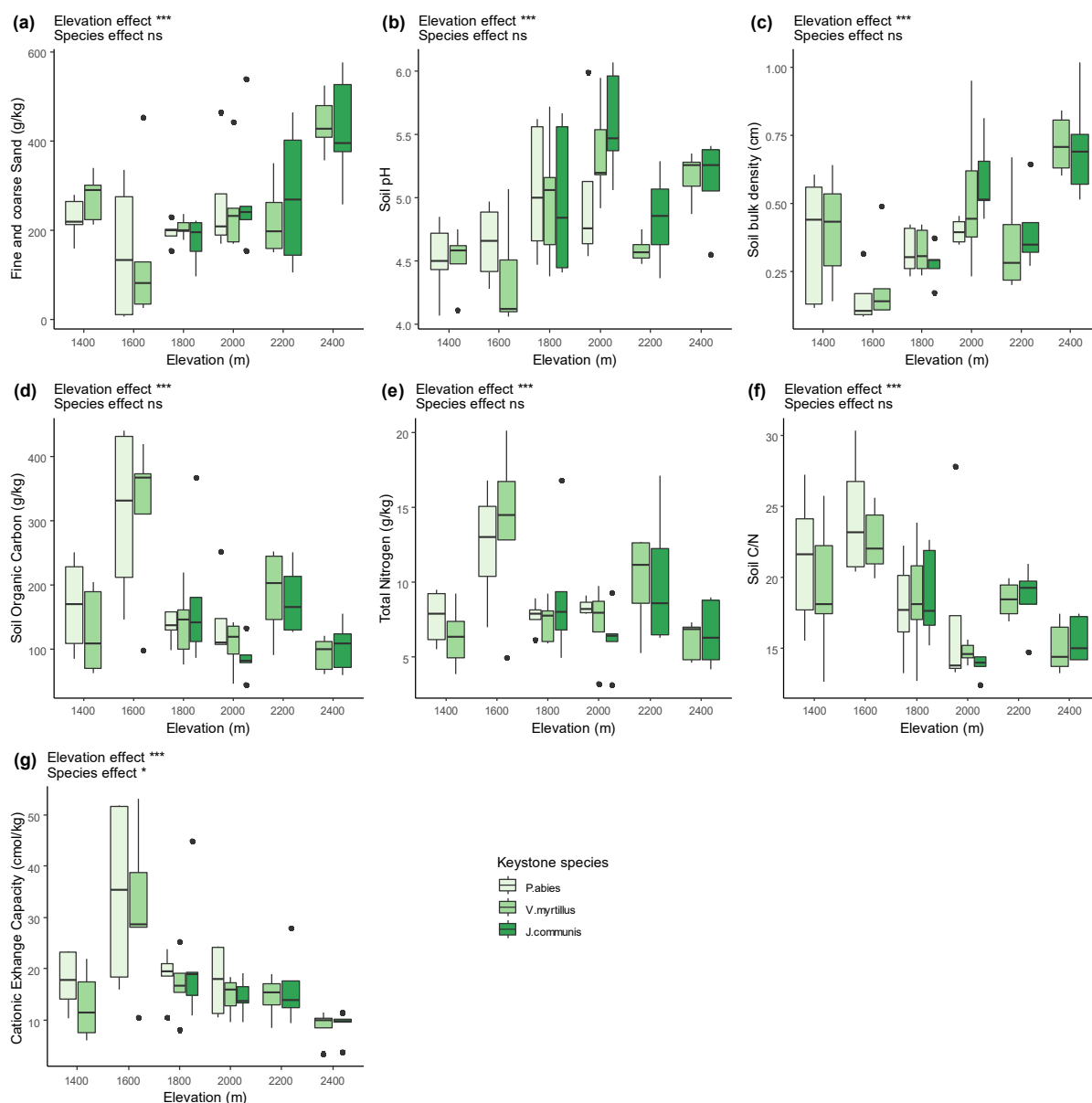


Figure S11: Differences in soil properties beneath keystone species and along the elevational gradient. (a) Soil sand content. (b) Soil pH measured in water. (c) Soil bulk density. (d) Soil organic carbon. (e) Total nitrogen. (f) Soil C to N ratio. (g) Soil cationic exchange capacity (Results of statistical WLS analyses are given in Table S6).

Table S7: PCA contributions (Contrib) and projection quality (Cos2) of the variables on the first two dimensions of the environmental PCA.

	Environmental PCA			
	Dimension 1		Dimension 2	
	0.46		0.23	
% variance	Contrib	Cos2	Contrib	Cos2
Bulk density	16.78	0.62	11.15	0.20
AI	15.85	0.59	7.8	0.14
Soil C : N	15.01	0.55	0.93	0.02
CEC	14.4	0.53	13.86	0.25
Sand	11.77	0.43	18.63	0.34
Herbaceous cover	9.18	0.34	15.51	0.28
MAT	8.77	0.32	19.25	0.35
Tree cover	8.25	0.31	12.87	0.23

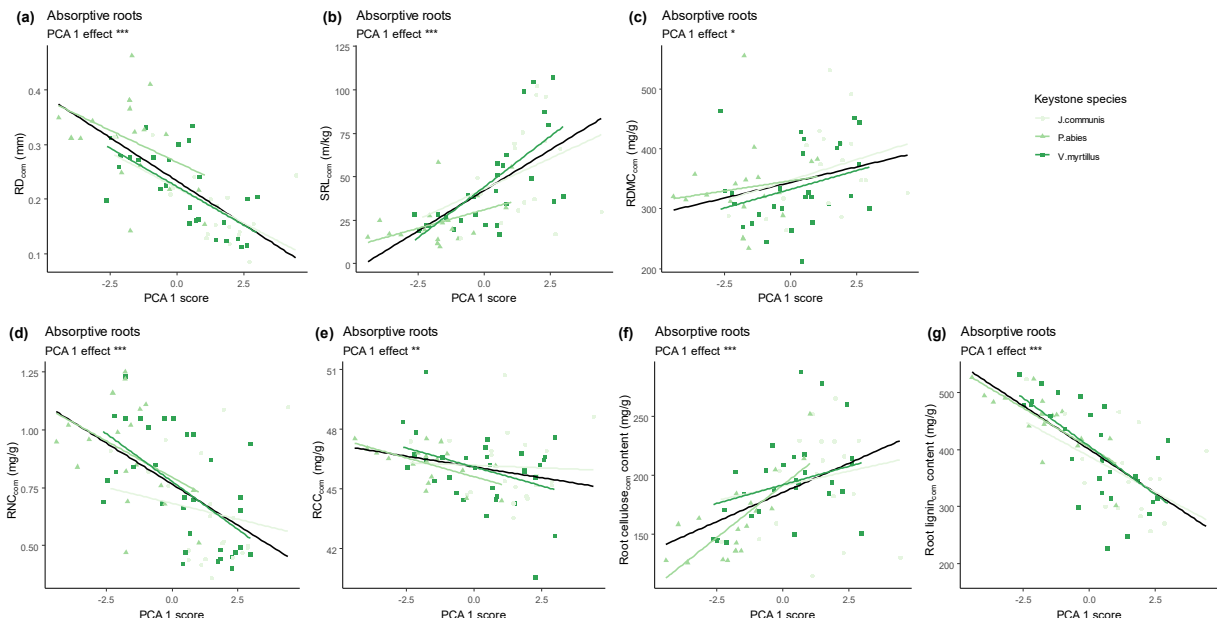


Figure S12: Variation in absorptive root traits_{com} along environmental PCA 1. Results are shown for root traits beneath each species (see legend). For abbreviations, see Table S5. Results of statistical WLS analyses are given in Table S5.

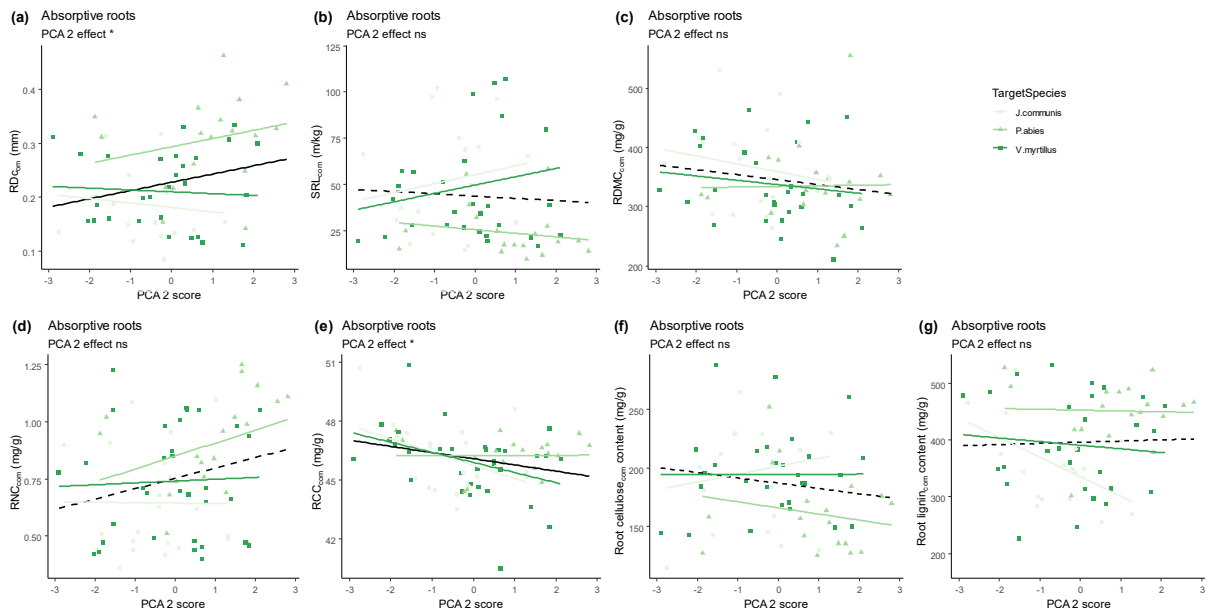


Figure S13: Variation in absorptive root traits_{com} along environmental PCA 2. Results are shown for root traits beneath each species (see legend). For abbreviations, see Table S5. Results of statistical WLS analyses are given in Table S5.

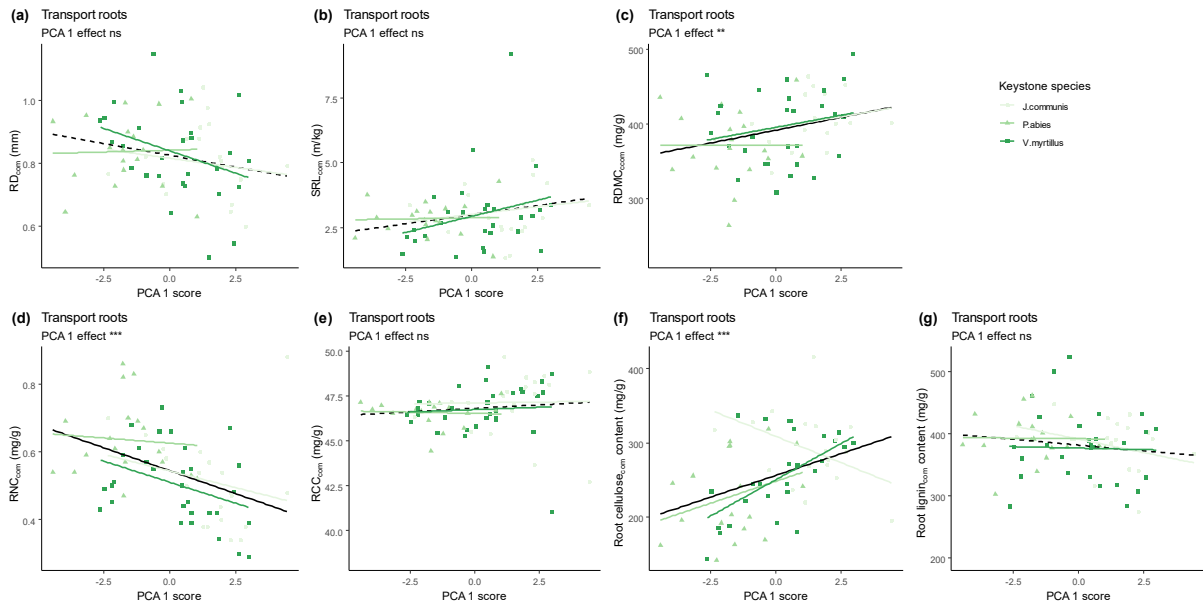


Figure S14: Variation in transport root traits_{com} along environmental PCA 1. Results are shown for root traits beneath each species (see legend). For abbreviations, see Table S5. Results of statistical WLS analyses are given in Table 3.

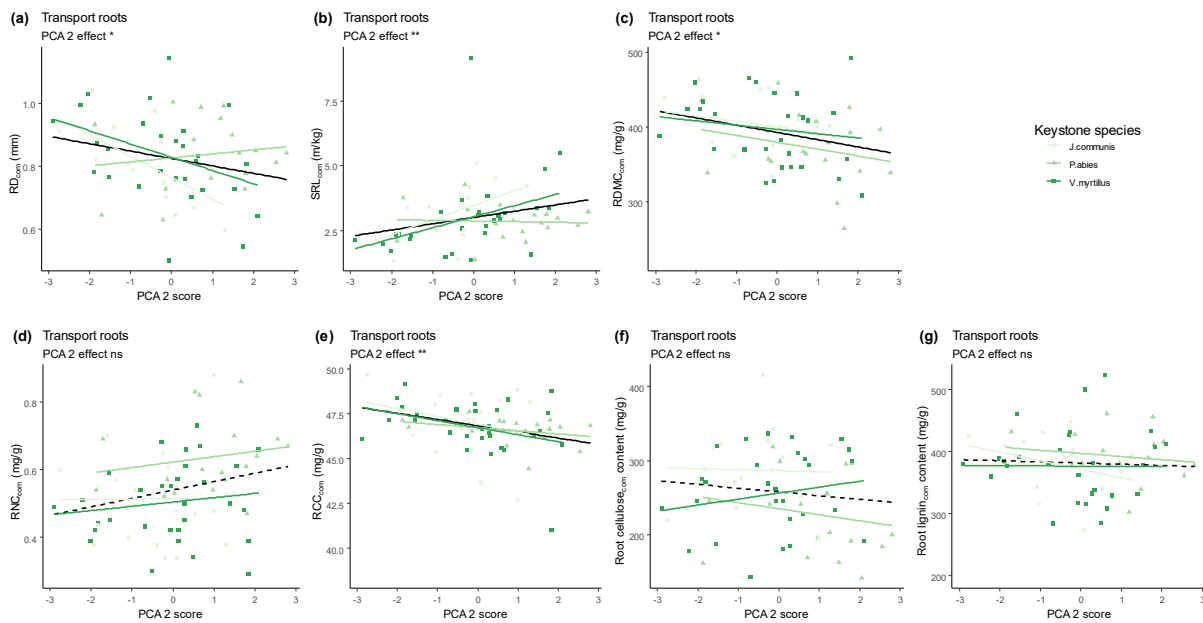


Figure S15: Variation in transport root traits_{com} along environmental PCA 2. Results are shown for root traits beneath each species (see legend). For abbreviations, see Table S5. Results of statistical WLS analyses are given in Table 3.

Table S8: PCA contributions (Contrib) and projection quality (Cos2) of the variables on the first two dimensions of the absorptive roots PCA and three first dimensions for transport roots.

	Absorption roots PCA				% variance	Transport roots PCA					
	Dimension 1		Dimension 2			Dimension 1		Dimension 2		Dimension 3	
	Contrib	Cos	Contrib	Cos		Contrib	Cos2	Contrib	Cos2	Contrib	Cos2
Lignin	21.17	0.84	2.90	0.04	SRL	39.48	0.84	3.27	0.06	1.20	0.01
RD	19.97	0.79	2.03	0.03	RD	32.58	0.70	8.62	0.15	2.15	0.03
SRL	17.94	0.71	0.87	0.01	RDMC	20.46	0.44	20.07	0.34	0.39	0.00
Cellulose	15.50	0.61	3.76	0.05	RNC	5.74	0.12	37.57	0.64	3.15	0.04
RNC	14.73	0.58	8.99	0.13	Lignin	1.06	0.02	8.42	0.14	55.09	0.65
RCC	5.79	0.23	33.08	0.46	Cellulose	0.58	0.01	18.46	0.32	20.16	0.24
RDMC	4.90	0.19	48.38	0.67	RCC	0.09	0.00	3.59	0.06	17.85	0.21

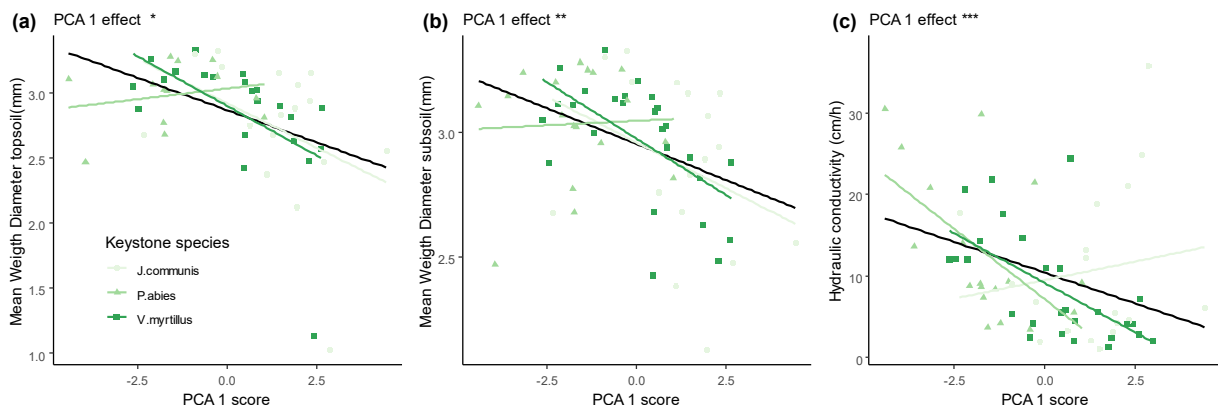


Figure S16: Soil processes along environmental PCA 1. Mean weight diameter of soil macro-aggregates collected in the topsoil and (b) in the subsoil, (c) Soil hydraulic conductivity (Results of statistical WLS analyses are given in Table 4).

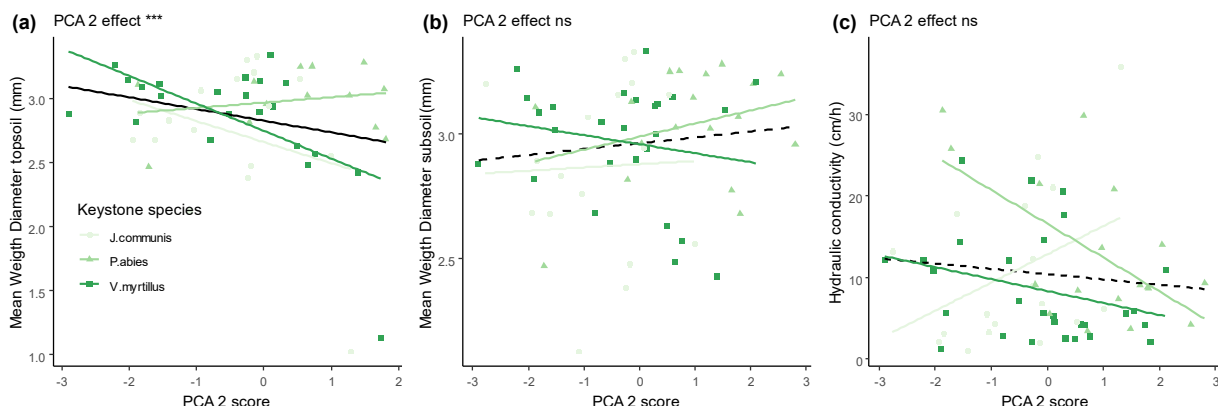


Figure S17: Soil processes along environmental PCA 2. Mean weight diameter of soil macro-aggregates collected in the topsoil and (b) in the subsoil, (c) Soil hydraulic conductivity (Results of statistical WLS analyses are given in Table 4).

References

- Ali H.E., Reineking B., & Münkemüller T. 2017. Effects of plant functional traits on soil stability: intraspecific variability matters. *Plant and Soil*. 411(1), p. 359-375.
- Bardat J., Bioret F., Botineau M., Boulet V., Delpech R., Géhu J.-M., Haury J., Lacoste A., Rameau J.-C., Royer J.-M., Roux G., & Touffet J. 2004. *Podrome des végétations de France*. Paris : Muséum national d'histoire naturelle, 171 p. (Patrimoines Naturels, 61)
- Barthès B. & Roose E. 2002. Aggregate stability as an indicator of soil susceptibility to runoff and erosion; validation at several levels. *CATENA*. 47(2), p. 133-149.
- Bast A., Wilcke W., Graf F., Lüscher P., & Gärtner H. 2014. The use of mycorrhiza for eco-engineering measures in steep alpine environments: effects on soil aggregate formation and fine-root development. *Earth Surface Processes and Landforms*. 39(13), p. 1753-1763.
- Bénichou P. & Lebreton O. 1987. Prise en compte de la topographie pour la cartographie des champs pluviométriques statistiques. *La Météorologie*. 7(23-24).
- Berendse F., Ruijven J. van, Jongejans E., & Keesstra S. 2015. Loss of Plant Species Diversity Reduces Soil Erosion Resistance. *Ecosystems*. 18(5), p. 881-888.
- Bjune A.E., Ohlson M., Birks H.J.B., & Bradshaw R.H.W. 2009. The development and local stand-scale dynamics of a *Picea abies* forest in southeastern Norway. *Holocene*. 19, p. 1073-1082.
- Blume-Werry G., Lindén E., Andresen L., Classen A.T., Sanders N.J., Oppen J. von, & Sundqvist M.K. 2018. Proportion of fine roots, but not plant biomass allocation below ground, increases with elevation in arctic tundra. *Journal of Vegetation Science*. 29(2), p. 226-235.
- Ciesielski H., Sterckeman T., Santerne M., & Willery J. 1997. A comparison between three methods for the determination of cation exchange capacity and exchangeable cations in soils. *Agronomie*. 17(1), p. 9-16.
- Dunne T., Zhang W., & Aubry B.F. 1991. Effects of Rainfall, Vegetation, and Microtopography on Infiltration and Runoff. *Water Resources Research*. 27(9), p. 2271-2285.
- Elrick D.E. & Reynolds W.D. 1992. Infiltration from Constant-Head Well Permeameters and Infiltrimeters. *Advances in Measurement of Soil Physical Properties: Bringing Theory into Practice*. sssaspecialpubl(advancesinmeasu), p. 1-24.
- Ennos A.R. & Pellerin S. 2000. Plant Anchorage. Dans : Smit A.L., Bengough A.G., Engels C., Van Noordwijk M., Pellerin Sylvain, Van de Geijn S.C. (éd.). *Root Methods: A Handbook*. Berlin, Heidelberg : Springer Berlin Heidelberg, p. 545-565.
- Erktan A., Cécillon L., Graf F., Roumet C., Legout C., & Rey F. 2016. Increase in soil aggregate stability along a Mediterranean successional gradient in severely eroded gully bed ecosystems: combined effects of soil, root traits and plant community characteristics. *Plant and Soil*. 398(1), p. 121-137.
- Freschet G.T. & Roumet C. 2017. Sampling roots to capture plant and soil functions. *Functional Ecology*. 31(8), p. 1506-1518.

- Freschet G.T., Valverde-Barrantes O.J., Tucker C.M., Craine J.M., McCormack M.L., Violle C., Fort F., Blackwood C.B., Urban-Mead K.R., Iversen C.M., Bonis A., Comas L.H., Cornelissen J.H.C., Dong M., Guo D., Hobbie S.E., Holdaway R.J., Kembel S.W., Makita N., Onipchenko V.G., Picon-Cochard C., Reich P.B., Riva E.G. de la, Smith S.W., Soudzilovskaia N.A., Tjoelker M.G., Wardle D.A., & Roumet C. 2017. Climate, soil and plant functional types as drivers of global fine-root trait variation. *Journal of Ecology*. 105(5), p. 1182-1196.
- Freschet G.T., Violle C., Bourget M.Y., Scherer-Lorenzen M., & Fort F. 2018. Allocation, morphology, physiology, architecture: the multiple facets of plant above- and below-ground responses to resource stress. *New Phytologist*. 219(4), p. 1338-1352.
- Fukami T. & Wardle D.A. 2005. Long-term ecological dynamics: reciprocal insights from natural and anthropogenic gradients. *Proceedings of the Royal Society B: Biological Sciences*. 272(1577), p. 2105-2115.
- Garcia M.C., Meneses R.I., Naoki K., & Anthelme F. 2014. Métodos para evaluar el efecto del pastoreo sobre las comunidades vegetales de bofedales. *Ecología en Bolivia*. 49(3), p. 91-103.
- Gerke H.H. & Kuchenbuch R.O. 2007. Root effects on soil water and hydraulic properties. *Biologia*. 62(5), p. 557-561.
- Ghestem M., Sidle R.C., & Stokes A. 2011. The Influence of Plant Root Systems on Subsurface Flow: Implications for Slope Stability. *BioScience*. 61(11), p. 869-879.
- Girardin C. & Mariotti A. 1991. Analyse isotopique du ¹³C en abondance naturelle dans le carbone organique: un système automatique avec robot préparateur. *Cahiers ORSTOM - Série Pédologie*. 26(4), p. 371-380.
- Gould I.J., Quinton J.N., Weigelt A., Deyn G.B.D., & Bardgett R.D. 2016. Plant diversity and root traits benefit physical properties key to soil function in grasslands. *Ecology Letters*. 19(9), p. 1140-1149.
- Hiraoka M. & Onda Y. 2012. Factors affecting the infiltration capacity in bamboo groves. *Journal of Forest Research*. 17(5), p. 403-412.
- Jonasson S. & Callaghan T.V. 1992. Root mechanical properties related to disturbed and stressed habitats in the Arctic. *New Phytologist*. 122(1), p. 179-186.
- Körner C. 1998. A re-assessment of high elevation treeline positions and their explanation. *Oecologia*. 115(4), p. 445-459.
- Körner C. 2007. The use of 'altitude' in ecological research. *Trends in Ecology & Evolution*. 22(11), p. 569-574.
- Körner C. & Renhardt U. 1987. Dry matter partitioning and root length/leaf area ratios in herbaceous perennial plants with diverse altitudinal distribution. *Oecologia*. 74(3), p. 411-418.
- Lado M., Paz A., & Ben-Hur M. 2004. Organic Matter and Aggregate-Size Interactions in Saturated Hydraulic Conductivity. *Soil Science Society of America Journal*. 68(1), p. 234-242.
- Laufen C.G., Chelsea, & Galerie. 2001. Flora Helvetica.

- Le Bissonnais Y., Prieto I., Roumet C., Nespoulous J., Metayer J., Huon S., Villatoro M., & Stokes A. 2018. Soil aggregate stability in Mediterranean and tropical agroecosystems: effect of plant roots and soil characteristics. *Plant and Soil*. 424(1), p. 303-317.
- Le Bissonnais Y., 1996. Aggregate stability and assessment of soil crustability and erodibility: I. Theory and methodology. *European Journal of Soil Science*. 47(4), p. 425-437.
- Lê S., Josse J., & Husson F. 2008. FactoMineR: An R Package for Multivariate Analysis. *Journal of Statistical Software*. 25(1), p. 1-18.
- Li F., Hu H., McCormack M.L., Feng D.F., Liu X., & Bao W. 2019. Community-level economics spectrum of fine-roots driven by nutrient limitations in subalpine forests. *Journal of Ecology*. 0(0).
- Mao Z., Wang Y., McCormack M.L., Rowe N., Deng X., Yang X., Xia S., Nespoulous J., Sidle R.C., Guo D., & Stokes A. 2018. Mechanical traits of fine roots as a function of topology and anatomy. *Annals of Botany*. 122(7), p. 1103-1116.
- Marín-Castro B.E., Negrete-Yankelevich S., & Geissert D. 2017a. Litter thickness, but not root biomass, explains the average and spatial structure of soil hydraulic conductivity in secondary forests and coffee agroecosystems in Veracruz, Mexico. *Science of The Total Environment*. 607-608, p. 1357-1366.
- McCormack M.L., Dickie I.A., Eissenstat D.M., Fahey T.J., Fernandez C.W., Guo D., Helmisaari H.-S., Hobbie E.A., Iversen C.M., Jackson R.B., Leppälammil-Kujansuu J., Norby R.J., Phillips R.P., Pregitzer K.S., Pritchard S.G., Rewald B., & Zadworny M. 2015. Redefining fine roots improves understanding of below-ground contributions to terrestrial biosphere processes. *New Phytologist*. 207(3), p. 505-518.
- Nespoulous J., Merino-Martin L., Monnier Y., Bouchet D., Ramel M., Dombey R., Viennois G., Mao Z., Zhang J.-L., Cao K., Le Bissonnais Y., Sirdle R.C., & Stokes A. 2019. Tropical forest structure and understorey determine subsurface flow through biopores formed by plant roots. *CATENA*.
- Nybakken L., Selås V., & Ohlson M. 2013. Increased growth and phenolic compounds in bilberry (*Vaccinium myrtillus* L.) following forest clear-cutting. *Scandinavian Journal of Forest Research*. 28(4), p. 319-330.
- Pansu M. & Gautheyrou J. 2006. *Handbook of Soil Analysis: Mineralogical, Organic and Inorganic Methods*. Berlin Heidelberg : Springer-Verlag
- Pérès G., Cluzeau D., Menasseri S., Soussana J.F., Bessler H., Engels C., Habekost M., Gleixner G., Weigelt A., Weisser W.W., Scheu S., & Eisenhauer N. 2013. Mechanisms linking plant community properties to soil aggregate stability in an experimental grassland plant diversity gradient. *Plant and Soil*. 373(1-2), p. 285-299.
- Piedallu C., Gégout J.-C., Lebourgeois F., & Seynave I. 2016. Soil aeration, water deficit, nitrogen availability, acidity and temperature all contribute to shaping tree species distribution in temperate forests. *Journal of Vegetation Science*. 27(2), p. 387-399.
- Piedallu C., Gégout J.-C., Perez V., & Lebourgeois F. 2013. Soil water balance performs better than climatic water variables in tree species distribution modelling. *Global Ecology and Biogeography*. 22(4), p. 470-482.

- Pohl M., Stroude R., Buttler A., & Rixen C. 2011. Functional traits and root morphology of alpine plants. *Annals of Botany*. 108(3), p. 537-545.
- Poirier V., Roumet C., & Munson A.D. 2018. The root of the matter: Linking root traits and soil organic matter stabilization processes. *Soil Biology and Biochemistry*. 120, p. 246-259.
- Rameau J.-C., Mansion D., & Dumé G. 1999. *Flore forestière française, Montagnes*. Institut pour le Développement Forestier
- Rillig M.C., Aguilar-Trigueros C.A., Bergmann J., Verbruggen E., Veresoglou S.D., & Lehmann A. 2015. Plant root and mycorrhizal fungal traits for understanding soil aggregation. *New Phytologist*. 205(4), p. 1385-1388.
- Six J., Conant R.T., Paul E.A., & Paustian K. 2002. Stabilization mechanisms of soil organic matter: Implications for C-saturation of soils. *Plant and Soil*. 241(2), p. 155-176.
- Stokes A., Douglas G.B., Fourcaud T., Giadrossich F., Gillies C., Hubble T., Kim J.H., Loades K.W., Mao Z., McIvor I.R., Mickovski S.B., Mitchell S., Osman N., Phillips C., Poesen J., Polster D., Preti F., Raymond P., Rey F., Schwarz M., & Walker L.R. 2014. Ecological mitigation of hillslope instability: ten key issues facing researchers and practitioners. *Plant and Soil*. 377(1), p. 1-23.
- Sundqvist M.K., Wardle D.A., Olofsson E., Giesler R., & Gundale M.J. 2012. Chemical properties of plant litter in response to elevation: subarctic vegetation challenges phenolic allocation theories. *Functional Ecology*. 26(5), p. 1090-1099.
- Tisdall J.M. & Oades J.M. 1982. Organic matter and water-stable aggregates in soils. *Journal of Soil Science*. 33(2), p. 141-163.
- Van Soest P.J. 1963. Use of detergents in the analysis of fibrous feeds. II. A rapid method for the determination of fiber and lignin. *Official agriculture Chemistry*. 46(829).
- Walsh R.D.P. & Voigt P.J. 1977. Vegetation litter an underestimated variable in hydrology and geomorphology. *Journal of Biogeography*. 4(3):253.
- Wardle D.A., Bardgett R.D., Klironomos J.N., Setälä H., Putten W.H. van der, & Wall D.H. 2004. Ecological Linkages Between Aboveground and Belowground Biota. *Science*. 304(5677), p. 1629-1633.
- Wu G.-L., Liu Y., Yang Z., Cui Z., Deng L., Chang X.-F., & Shi Z.-H. 2017. Root channels to indicate the increase in soil matrix water infiltration capacity of arid reclaimed mine soils. *Journal of Hydrology*. 546, p. 133-139.
- Wu L. & Pan L. 1997. A Generalized Solution to Infiltration from Single-Ring Infiltrimeters by Scaling. *Soil Science Society of America Journal*. 61(5), p. 1318-1322.
- Wu L., Pan L., Mitchell J., & Sanden B. 1999. Measuring Saturated Hydraulic Conductivity using a Generalized Solution for Single-Ring Infiltrimeters. *Soil Science Society of America Journal*. 63(4), p. 788-792.
- Zadworny M., McCormack M.L., Żytkowiak R., Karolewski P., Mucha J., & Oleksyn J. 2017. Patterns of structural and defense investments in fine roots of Scots pine (*Pinus sylvestris* L.) across a strong temperature and latitudinal gradient in Europe. *Global Change Biology*. 23(3), p. 1218-1231.